

# Homology Modeling of the Dopamine D<sub>2</sub> Receptor and Its Testing by Docking of Agonists and Tricyclic Antagonists

Martha M. Teeter,<sup>\*†</sup> Mark Froimowitz,<sup>‡,⊥</sup> Boguslaw Stec,<sup>†</sup> and Curtiss J. DuRand<sup>§,||</sup>

Eugene F. Merkert Chemistry Center, Department of Chemistry, Boston College, Chestnut Hill, Massachusetts 02167, and Alcohol and Drug Abuse Research Center and Department of Psychiatry, McLean Hospital, Harvard Medical School, Belmont, Massachusetts 02178

Received April 4, 1994<sup>⊗</sup>

We present the first model of dopamine D<sub>2</sub> receptor transmembrane helices constructed directly from the bacteriorhodopsin (bR) coordinates derived from two-dimensional electron diffraction experiments. We have tested this model by its ability to accommodate rigid agonist and semirigid antagonist molecules which were docked into the putative binding pocket with stabilizing interactions. The model is consistent with structure–activity relationships of agonists and antagonists that interact with the receptor. It also illuminates data on a Na<sup>+</sup> site for regulation of receptor function. The plausibility of the model is increased by its consistency with many mutagenesis studies on G protein-coupled receptors. Further, this model provides a basis to suggest testable molecular mechanisms for changes in the D<sub>2</sub> conformational states for high- and low-affinity binding and signal transduction. Changes in the conformational state of the receptor are hypothesized to be due partly to movement of helix 7. In contrast to the model presented here, other published models were built using ideal helical structures or following the sense of the bacteriorhodopsin structure rather than the actual available coordinates. The presented model for the dopamine G protein-coupled receptor can be reconciled with the recent rhodopsin projection structure (Schertler, G. F. X.; Villa, C.; Henderson, R. Projection Structure of Rhodopsin. *Nature* **1993**, *362*, 770–772).

## Introduction

G protein-coupled receptors constitute a superfamily of up to 1000 or 2000 integral membrane proteins constituting 1–2% of all genes. It is arguably the largest gene family for any protein family. In fact, 80% of all hormone and neurotransmitter receptor subtypes are G protein-coupled receptors.<sup>1</sup> Included in this family<sup>2–4</sup> are adrenergic, dopaminergic, serotonergic, and muscarinic receptors, receptors for peptides, odorants, opsins, and related receptors.<sup>5</sup> Their function is to mediate communication between cells by receiving first messenger signals from neurotransmitters, hormones, photons, odorants, or pheromones and transducing those signals by activating intracellular G proteins.<sup>6</sup>

Knowledge of the three-dimensional structure of these receptors is expected to improve our understanding of the neurochemistry and molecular pathology of disease and to facilitate development of improved therapeutic agents. Specifically, efficacy of drugs used to treat schizophrenia has been tied to their binding affinity for dopamine D<sub>2</sub> receptors, the subject of this report.<sup>7,8</sup>

Hydrophobicity plots and other data support the notion that G protein-coupled receptors contain seven hydrophobic transmembrane regions. The recent cloning and sequencing of many of these receptors<sup>3,9</sup> combined with biochemical and pharmacological studies of

opsins and monoaminergic receptors<sup>10–14</sup> provides substantial data for prediction of their three-dimensional structure and function.

This three-dimensional structure prediction is greatly aided by the superfamily's relationship to bacteriorhodopsin, the photon-driven hydrogen ion pump whose three-dimensional structure is known to the nominal resolution of 3.5 Å.<sup>2,15,16</sup> This protein is similar to rhodopsin with which it shares the binding of retinal and a similar topology of seven transmembrane helices. On the basis of the hypothesized *structural* homology of bacteriorhodopsin with rhodopsin, a number of models of G protein-coupled receptors have been built,<sup>17–22</sup> even though the receptors have little *sequence* homology. These models have been based to a greater or lesser extent on the bacteriorhodopsin structure, but all employ theoretical methods such as ideal helices and molecular dynamics.

Experience with high-resolution protein structure<sup>23,24</sup> has made the authors aware of the importance of diffraction data and the use of homology relationships<sup>25</sup> in constructing a model. Presented here is the first model of the dopamine D<sub>2</sub> receptor constructed directly from the coordinates of the bacteriorhodopsin structure. Further, this model has been tested by its ability to rationalize drug binding data and to explain the effect of Na<sup>+</sup> on receptor activity. Finally, mutagenesis studies add further credence to the model.

To test the drug binding site of the receptor, we chose the direct approach of docking ligands whose conformational freedom is limited<sup>26–29</sup> and thus whose active conformations are established. There is considerable information available on the structure–activity relationships of dopamine agonists and antagonists, and an accurate dopamine receptor model should be consistent with these relationships.

\* Author to whom inquiries should be addressed: e-mail to teeter@bcchem.bc.edu.

† Boston College.

‡ Alcohol and Drug Abuse Research Center, Harvard Medical School.

§ Department of Psychiatry, Harvard Medical School.

⊥ Present address: Pharm-Eco Laboratories, 128 Spring St., Lexington, MA 02173.

|| Present address: ENRM VA Medical Center, 200 Springs Rd., Bedford, MA 01730.

⊗ Abstract published in *Advance ACS Abstracts*, July 15, 1994.

In dopamine agonists, considerable steric bulk in the N-substituent can be accommodated in one direction but not another.<sup>27,29</sup> For dopamine antagonists, the situation is less clear since most antagonists have considerable conformational flexibility. However, a number of semirigid compounds have been identified and used to define a pharmacophore for dopamine antagonism.<sup>28,30,31</sup> Features identified as being important include both a particular curvature of the tricyclic structure that is present in all tricyclic antagonists and the required orientation of the ammonium hydrogen. Another feature that is crucial for high-affinity binding in almost all dopaminergic antagonists is the presence of a substituent on a phenyl ring as exemplified by the 2-Cl group in chlorpromazine and loxapine, a 2-CF<sub>3</sub> group in fluphenazine, and a 2-SCH<sub>3</sub> group in thioridazine.<sup>32</sup> The distance of the center of this ring to the ammonium nitrogen is approximately 6.2 Å in typical D<sub>2</sub> antagonists.<sup>28</sup>

A model should be able to illuminate other features of the receptor, such as the relative activity of structurally related agonists/antagonists and the influence of Na<sup>+</sup> and pH on agonist/antagonist binding. Neve<sup>33,34</sup> has shown a pivotal role for an Asp on helix 2 in regulation of D<sub>2</sub> affinity for drugs, coupling to adenylate cyclase, and sensitivity to Na<sup>+</sup> and pH. Because of these and related reports<sup>35,36</sup> as well as the very high conservation of this residue in the super-family of G protein-coupled receptors,<sup>5</sup> its role in sodium and drug binding was explored. Sodium decreases the binding of D<sub>2</sub> agonists and increases the binding of some substituted benzamides but not other D<sub>2</sub> antagonists. Neve concludes that Na<sup>+</sup> and H<sup>+</sup> regulate the conformation of D<sub>2</sub> receptors. pH changes could induce conformational changes in receptor state via residue ionization, and Na<sup>+</sup> and H<sup>+</sup> could bind to a site on D<sub>2</sub> to regulate its conformational state, as demonstrated for α<sub>2</sub> adrenergic receptors.<sup>35</sup>

Mutagenesis of the cloned dopamine and related monoaminergic receptors combined with drug binding experiments can spotlight the most important residues for primary signal binding. Certain receptor residues have been identified previously as directly interacting with catecholamine agonists, namely two Ser residues on helix 5 to hydrogen bond to dopamine's catechol hydroxyls and an Asp on helix 3 to salt bridge with the ammonium nitrogen. However, a large amount of mutagenesis data suggests the importance of other residues in ligand binding, perhaps through van der Waals contacts and hydrogen-bonding interactions. The ability to rationalize this data can significantly strengthen the power of a receptor model.

The model is contrasted with others. It is also used to illuminate an assignment of helices to the recent low-resolution projection structure of rhodopsin.<sup>37</sup> Agonist binding indicates dopamine receptors exist in both a high- and low-affinity state. The origin of the change in conformation of the receptor is hypothesized.

## Methods

**Construction of the Model.** Protein crystallographic data support the notion that there are a small number of structural motifs in proteins and that the same structural motif or fold can be used for nonhomologous sequences, e.g., the β-barrel fold,<sup>38</sup> or from low homology sequences, e.g., the globin fold.<sup>38</sup> This notion is applied to the present bacteriorhodopsin-based model of the D<sub>2</sub> receptor.

The approach to modeling the tertiary structure of the dopamine D<sub>2</sub> receptor described here is based directly on structural and functional data which has been experimentally obtained, namely the three-dimensional structure of bacteriorhodopsin from electron diffraction experiments by Henderson and co-workers<sup>15</sup> together with ligand binding mutagenesis data. In contrast, previous attempts<sup>17-22</sup> have used a more theoretical approach, such as building ideal helices or following the "sense" but not the details of known crystal structures of membrane proteins.

### Use of Crystal Coordinates and Sequence Alignment.

There are compelling reasons for using the known coordinates of bacteriorhodopsin<sup>15</sup> to generate models of G protein-coupled receptors such as rhodopsin and D<sub>2</sub> receptors. Although the sequence identity of bacteriorhodopsin with G-protein coupled receptors is only 6–11%,<sup>19</sup> they appear to have the same fold for the transmembrane helical segments.<sup>2</sup> Further, in both bacteriorhodopsin and opsin, (1) the chromophore is attached to a comparable Lys residue in the center of the 7th helix; (2) the topological orientation of the helices in the plasma membrane is the same; (3) energy generated by a photon is the same and photons induce retinal isomerization and protein conformational changes in both; and (4) proteolytic cleavage at hydrophilic sites does not abolish electrogenic activity.<sup>16</sup> Even further, retinal shares structural properties with receptor agonists such as biogenic amines and acetylcholine.<sup>2</sup>

In order to optimize the alignment of bacteriorhodopsin with the D<sub>2</sub> receptors, representatives of the catecholaminergic G protein-coupled receptors were used: rhodopsin, β<sub>2</sub>-adrenergic, and dopamine D<sub>2</sub> receptors. In this way, the functional similarities between bacteriorhodopsin and rhodopsin<sup>2,16</sup> could be used to advantage as well as mutational data on critical binding pocket residues in β<sub>2</sub>-adrenergic receptors.<sup>11,12</sup>

Our hand alignment of amino acid sequences of rhodopsin, β<sub>2</sub>-adrenergic, and dopamine G protein-coupled receptors (Table 1) was found to be identical to that of others.<sup>5</sup> This sequence alignment seems to be generally agreed upon.<sup>21,39</sup> It is given even more validity in light of the superfamily alignment for a large number of known sequences of these receptors, including the monoaminergic, peptide receptors, and sensory receptors.<sup>5</sup>

Once the alignment of bacteriorhodopsin and the G protein-coupled receptors was established (see below), bacteriorhodopsin residue numbers were used for all receptors. That convention will be followed throughout this paper (Table 1). In addition, the helix that contains a residue will be identified by the number corresponding to the bacteriorhodopsin helical fold. Where clarity is served, a statement will be made of the original numbering for a given residue.

### Use of Helical Wheel/Nonpolar Faces in Helix Alignment with Bacteriorhodopsin.

Helical wheels<sup>40</sup> were used to align sequences of bacteriorhodopsin's transmembrane helical regions with the G protein-coupled receptors. These wheels display helix residues projected down the helical axis so that the amphipathicity—the separation of nonpolar and polar residues—is apparent. First, helical wheels for bacteriorhodopsin (Figure 1a) were constructed using a projection diagram of the electron microscopy structure.<sup>15</sup> Next, the helical wheels of bacteriorhodopsin were analyzed to determine which residues face the lipid alkyl chains, i.e., are in the nonpolar faces. In addition to the clearly hydrophobic residues (Leu, Ile, Val, Phe), the residues found on this face included Thr, Tyr, Ala, and Gly. Polar or charged residues within one helical turn of the end of the helix were not included as defining rules for this face, since they could associate with turns, lipid head groups, or other hydrophilic molecules.

Helical wheels were then constructed for each G protein-coupled receptor (rhodopsin, β<sub>2</sub>-adrenergic, and D<sub>2</sub>) from the two-dimensional helical wheel template of the bacteriorhodopsin structure. Using the rules derived above to define nonpolar faces, the helical wheels were rotated to orient the nonpolar faces similarly to bacteriorhodopsin and toward the lipid alkyl chains, at first for each receptor independently and then to agree with the sequence alignment for all the G protein-coupled receptors.<sup>5</sup> This method resulted in good sequence alignment for helices 1, 2, 4, 5, and 6 from a comparison with bacteriorhodopsin nonpolar faces and conservation of important drug binding residues (Sers and Asp, see above). This

**Table 1.** Sequence Alignment for Bacteriorhodopsin (bR), Rhodopsin,  $\beta_2$  Adrenergic, and D<sub>2</sub> Receptors<sup>a</sup>

HELIX 1: residues 9-33				
	9		19	29
bR	9	EWIWLALGTA	LMGLGTLYFL	VKGMG 33
Rhod	37	FSMLAAYMFL	LEVLGFPINF	LTLYV 61
$\beta_2$ ar	33	VVGMGIVMSL	IVLAIVFGNV	LVITA 57
D <sub>2</sub>	34	YNYATLLTL	LIAVIVFGNV	LVCMA 58
HELIX 2: 38-63				
	38		48	58
bR	38	DAKKFYAITT	LVPPIAFTMY	LSMLLG 63
Rhod	75	ILLNLAVADL	FMVLGGFTST	LYTSLH 100
$\beta_2$ ar	71	FITSLACADL	VMGLAVVPPG	AAHILM 96
D <sub>2</sub>	72	LIVSLAVADL	LVATLVMPWV	VYLEV 97
HELIX 3: 80-101				
	80		90	100
bR	79	Y WARYADWLFT	TPLLLDLAL	LVDADQ 105
Rhod	110	C NLEGGFATLG	GEIALQSLVV	LAIERY 136
$\beta_2$ ar	106	C EFWTSIDVLC	VTASITLCV	IAVDRY 132
D <sub>2</sub>	107	C DIFVTLDMVM	CTASILNLCA	ISIDRY 133
HELIX 4: 108-127				
	108		118	
bR	108	ILALVGADGI	MIGTGLVGAL	127
Rhod	154	IMGVAFVWM	ALACAAPPLA	173
$\beta_2$ ar	151	RVIIIMVWIV	SGLTSFLPIQ	170
D <sub>2</sub>	153	TVMISIVWVL	SFTISCPPLF	172
HELIX 5: 137-157				
	137		147	157
bR	137	WWAISTAAML	YILYVLFPGF	T 157
Rhod	204	VYMFVVHFT	IPMIIIFCY	G 224
$\beta_2$ ar	200	AIASSIVSFY	VPLVIMVFVY	S 220
D <sub>2</sub>	190	VVYSSIVSFY	VPFIVTLLVY	I 210
HELIX 6: 167-192				
	167		177	187
bR	167	VASTFKVLRN	VTVVLWSAYP	VVWLIG 192
Rhod	250	VTRMVIIMVI	AFLICWVPYA	SVAFYI 275
$\beta_2$ ar	271	ALKTLGIIMG	TFTLCWLPFF	IVNIVH 296
D <sub>2</sub>	342	ATQMLAIVLG	VFIIICWLPFF	ITHILN 367
HELIX 7: 203-226				
	203		213	223
bR	203	IETLLFMVLD	VSAKVGFLI	LLRS 226
Rhod	283	FGPIFMTIPA	FFAKSAAIYN	PVIY 306
$\beta_2$ ar	303	IRKEVYILLN	WIGYVNSGFN	PLIY 326
D <sub>2</sub>	374	IPPVLYSAFT	WLGYVNSAVN	PIIY 397

<sup>a</sup> Bacteriorhodopsin numbering is indicated above each line. Henderson, R.; Baldwin, J. M.; Ceska, T. A. Model for the Structure of Bacteriorhodopsin based on High-resolution Electron Cryo-microscopy. *J. Mol. Biol.* **1990**, *213*, 899-929. Nathans, J.; Hogness, D. S. Isolation and nucleotide sequence of the gene encoding human rhodopsin. *Proc. Natl. Acad. Sci. U.S.A.* **1984**, *81*, 4851-4855. Koblika, B. K.; Dixon, R. A. F.; Friele, T.; Dohlman, H. G.; Bolanowski, M. A.; Sigal, I. S.; Yang, Feng, T. L.; Francke, U.; Caron, M. G.; Lefkowitz, R. J. cDNA for the human beta2-adrenergic receptor: a protein with multiple membrane spanning domains and encoded by a gene whose chromosomal location is shared with that of the receptor for platelet-derived growth factor. *Proc. Natl. Acad. Sci. U.S.A.* **1987**, *84*, 46-50. Bunzow, J. R.; Van Tol, H. H. M.; Grandy, D. K.; Albert, P.; Salon, J.; MacDonald, C.; Machida, C. A.; Neve, K. A.; Civelli, O. Cloning and expression of a rat D2 dopamine receptor cDNA. *Nature* **1988**, *336*, 783-787. Grandy, D. K.; Marchionni, M. A.; Makam, H.; Stofko, R. E.; Alfano, M.; Frothingham, L.; Fischer, J. B.; Burke-Howie, K. J.; Bunzow, J. R.; Server, A. C.; Civelli, O. Cloning of the cDNA and gene for a human D2 dopamine receptor. *Proc. Natl. Acad. Sci. U.S.A.* **1989**, *86*, 9762-9766. Dal Toso, R.; Sommer, B.; Ewert, M.; Herb, A.; Pritchett, D. B.; Bach, A.; Shivers, B. D.; Seeburg, P. H. The dopamine D2 receptor: two molecular forms generated by alternative splicing. *EMBO J.* **1989**, *8*, 4025-4034. Shichi, H. Molecular Biology of Vision. In *Basic Neurochemistry*; Siegel, G. J., Agranoff, B. W., Albers, W. R., Molinoff, P. B., Eds.; Raven Press: New York, 1994; p 1080.

was not true for helices 3 and 7, based on the tests described below of agonist docking and violations of the nonpolar faces.

For helix 3, mutagenesis studies of the  $\beta_2$ -adrenergic receptor ( $\beta_2$ ar) suggested that (1) the quaternary amine of epinephrine as well as that of other  $\beta_2$ ar ligands interacts with the carboxylate group of Asp113 ( $\beta_2$ ar numbering) on helix 3<sup>11</sup> and (2) the *m*- and *p*-hydroxyl groups of epinephrine form hydrogen

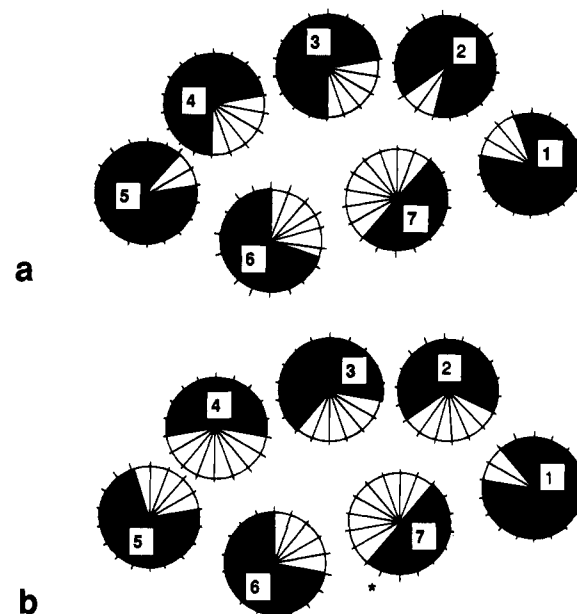


**Figure 1.** Nonpolar faces of bacteriorhodopsin and the dopamine D<sub>2</sub> receptor model in the helical wheel representation. The bacteriorhodopsin faces were derived from the crystallographic data and the receptor model were matched to it. See text.

bonds with Ser204 and Ser207 ( $\beta_2$ ar numbering) on helix 5, respectively.<sup>12</sup> These residues correspond to Asp86, Ser141, and Ser144 in the D<sub>2</sub> receptor, using bacteriorhodopsin numbering.

To test this for our initial model, the active *trans* conformer of dopamine<sup>41,42</sup> was docked to the corresponding residues in the bacteriorhodopsin-aligned D<sub>2</sub> receptor (see below for model building). The Ser to Asp distance was too long for dopamine and apomorphine to bind to the Ser O<sub>γ</sub> and Asp O<sub>δ1</sub> simultaneously until we realigned helix 3 by one residue. This realignment brought Trp86 in bacteriorhodopsin (helix 3) into register with Asp114 in D<sub>2</sub> numbering or Asp113 for  $\beta_2$ ar, instead of Asp85 in bacteriorhodopsin with the above Asps in the receptors. Both Asp85 and Trp86 are in the retinal binding pocket and proton channel of bacteriorhodopsin (Table 2). Thus either alignment shows correspondence between active bacteriorhodopsin residues and active D<sub>2</sub> residues.

In helix 7, no alignment was clearly favored. Therefore, the sequences of the G protein-coupled receptors were shifted systematically relative to bacteriorhodopsin, and the number of hydrophobicity violations was counted. (A violation would have a polar residue where the bacteriorhodopsin nonpolar face was located.) Ultimately, the alignment chosen has Lys216 from bacteriorhodopsin aligned with the comparable Lys in rhodopsin to which retinal is attached in both. One violation occurred (Asn218, using bacteriorhodopsin numbering, see Figure 1b) on the receptor hydrophobic face.

The resulting alignment of the G protein-coupled receptors with bacteriorhodopsin is shown in Table 1.

**Building a Three-Dimensional Model for the Dopamine D<sub>2</sub> Receptor.** The deposited coordinates (1BRD.BRK) of bacteriorhodopsin<sup>15</sup> from the Protein Data Bank<sup>43,44</sup> were used to construct a three-dimensional model of the D<sub>2</sub> receptor. Helix 4 was moved in the positive *z* direction by ~3.8 Å in a later model revision (R. Henderson, personal communication, 1993). Four main steps were used: amino acid substitution, local geometry optimization, Pro replacements, and side-chain rotation to minimize overlaps between helices. The initial procedure involved the interactive graphics program FRODO<sup>45</sup> First, amino acids in the dopamine D<sub>2</sub> were substituted for those in bacteriorhodopsin. Local Hermann's energy minimization for 20 cycles made substituted coordinates real and constrained them to ideal local geometry.

Since it was known that the helices in bacteriorhodopsin are kinked from 10° to 30° at Pro residues,<sup>15</sup> the problem was to remove these kinks where Pros were not present in the G-protein coupled receptors and introduce new ones where

**Table 2.** Comparison of Selected Residues between the Presented D<sub>2</sub> Model and Henderson's Model of Bacteriorhodopsin<sup>a</sup>

bacteriorhodopsin	D <sub>2</sub> model	D <sub>2</sub> short numbering
Binding Pocket		
Arg82 (p) <sup>b</sup>	Phe82	Phe110
Trp86 (rp)	Asp86	Asp114
Thr90 (r)	Cys90	Cys118
Asp115 (r)	Trp115	Trp160
Met118 (r)	Ser118	Ser163
Gly122 (r)	Ser122	Ser167
Ser141 (r)	Ser141	Ser194
Ala144	Ser144	Ser197
Met145 (r)	Phe145	Phe198
Trp182 (r)	Trp182	Trp357
Tyr185 (r)	Phe185	Phe360
Pro186 (r)	Phe186	Phe361
Ancillary Pocket		
Met56	Trp56	Trp90
Thr89 (rp)	Met89	Met117
Arg82 (p)	Phe82	Phe110
Phe208 (p)	Tyr208	Tyr379
Asp212 (rp)	Thr212	Thr383
Lys216 (rp)	Tyr216	Tyr387
Sodium Site		
Phe27	Asn27	Asn52
Thr46 (p)	Asp46	Asp80
Leu93 (rp)	Ser93	Ser121
Asp96 (p)	Asn96	Asn124
Phe219 (p)	Ser219	Ser390
Ile222 (p)	Asn222	Asn393

<sup>a</sup> Henderson, R.; Baldwin, J. M.; Ceska, T. A. Model for the Structure of Bacteriorhodopsin Based on High-resolution Electron Cryo-microscopy. *J. Mol. Biol.* **1990**, *213*, 899–929. <sup>b</sup> r = retinal pocket residue; p = proton channel residue.

they were found. Several templates exist for backbone angle changes around a Pro.<sup>46,47</sup> However, results with these did not give compact structures. Idealizing helix backbone angles where Pro's were removed also did not work. Ideal helix angles tended to produce a helix that was too long, i.e., the rise/turn was greater than that found in the experimentally obtained bacteriorhodopsin structural data. This would be a hazard of using automated modeling packages to build helices. Real helices may "average" to the ideal value but deviate significantly along the chain.

Therefore, assuming that the data-based helices from bacteriorhodopsin coordinates might be more accurate than those of the averaged Pro-containing structures, a template was designed for helical Pro residues by combining residues 38–63 and 80–101 from helices 2 and 3, respectively (bacteriorhodopsin numbering). The changed prolines had the closest intramolecular contacts in the initial model (Pro55 added and Pro50 removed, Pro148 and Pro150 added in helix 5, Pro186 removed, and Pro184 added in helix 6). The changed Pros were in the middle of helices or near the binding pocket. Terminal Pros 204, 205, and 223 were not changed, which may contribute to problems (see below) for helix 7 modeling. Terminal Pros were difficult to change objectively because they change the entire helix packing.

A rotamer library (a data base of preferred side chain torsion angles) has been developed from protein X-ray structures for hydrophilic proteins.<sup>48</sup> The program CHAIN,<sup>49</sup> derived from FRODO, incorporates these rotamer preferences and was used to manually construct the best side chain angles for the helices and remove close contacts before global minimization. Close contacts were also detected by running an independent program (PROLSQ) to identify short van der Waals distances.

**Why Global Energy Minimization Was Not Used for the Final Model.** The prior experience of one author<sup>24</sup> was that energy minimization can move a protein structure away from its well-determined crystal structure (namely crambin at 0.945-Å resolution). The distortions were often disturbingly systematic (all  $\Phi$  angles changed in the same direction).<sup>24</sup> This has been born out also by X-ray refinement of crambin where potential energy functions were used (X-PLOR refinement, A.

Yamano and M. M. Teeter, unpublished results). With intermediate models of the dopamine D<sub>2</sub> receptor, energy minimization resulted in distorted peptide bond torsion angles ( $\omega$ ), which were 10–20° away from 180°, the accepted value. Usual variation is  $\pm 5^\circ$  from 180°. Even a few short van der Waals contacts resulted in a very distorted structure.

Thus it was decided that the D<sub>2</sub> receptor model most true to the bacteriorhodopsin data would not have global energy minimization but minimal close van der Waals contacts. The major changes made from bacteriorhodopsin thus were local energy minimization, Pro adjustment, and rotation about side-chain torsion angles (after suitable residue substitutions). These procedures resulted in removal of most close contacts.

**Construction of Ligand Coordinates and Method of Docking.** The active conformations of agonists and antagonists were derived from crystal coordinates of molecular mechanics calculations.<sup>28,31,41,42</sup> For ligands not previously studied (trifluoperazine, fluphenazine, and *N-n*-butylnorapomorphine), molecular mechanics minimized conformations which were closest to the previously established pharmacophore were used.<sup>28,31</sup>

Agonist docking was typified by dopamine. It was docked to form a salt bridge between the ammonium nitrogen and Asp86 on helix 3. Simultaneously, good hydrogen bonds could be formed with the *m*- and *p*-OH groups of dopamine to Ser141 and Ser144, respectively, on helix 5. Other agonists were docked independently by establishing bonds between the corresponding portions of the ligands and the same residues in the receptor. Their final positions agreed well (Figure 2).

All antagonists had ammonium nitrogens in an analogous position to dopamine and the other agonists. In addition, some had potential hydrogen bonding groups in the central ring of the tricyclic system. In these cases, Asp86 and Ser141 were found to be the target points for bonding which resulted in the least van der Waals overlap. Adjustments were made in side-chain conformations of the bonding residues, conformations of aromatic residues in the binding pocket, and ligand positions in order to optimize bonding geometry, to relieve close van der Waals contacts, and to fill the available space.

Separate models were built for receptors with agonists and with antagonists. Some side chain conformations were different for each.

## Results of Docking

**The Agonist Binding Site: Agonists Dock Perpendicular to the Membrane Plane.** The two dopamine hydroxyl groups hydrogen bond to two Ser residues on helix 5 (Ser141 and Ser144). These are located on helix turn away or approximately over one another when the receptor is viewed down the helix axes (Figure 2). This means that the aromatic ring plane of dopamine is aligned parallel to the transmembrane helix axes and perpendicular to the membrane plane (Figure 3).

The analog of apomorphine with an *N-n*-propyl group has high affinity for dopamine receptors, but larger groups such as *N*-isobutyl and *N*-isopropyl result in an almost complete loss of receptor affinity.<sup>50</sup> In contrast, in octahydrobenzo[*f*]quinolines in which the N-group substituent projects in a different direction, groups as large as phenethyl can be easily accommodated without a loss of dopaminergic activity.<sup>51</sup> These compounds provide good measuring sticks for evaluating the drug binding pocket.

In order to test whether the model could explain these differences, relevant members of the apomorphine family were docked into the D<sub>2</sub> receptor. Since the agonist apomorphine and its derivatives have four rings whose mean plane is close to the phenyl ring of dopamine, these too lie parallel to the helix axes (Figure 2). A salt bridge was made between the quaternary nitrogen and Asp86 (helix 3). High affinity for the D<sub>2</sub> receptor of 0.7–

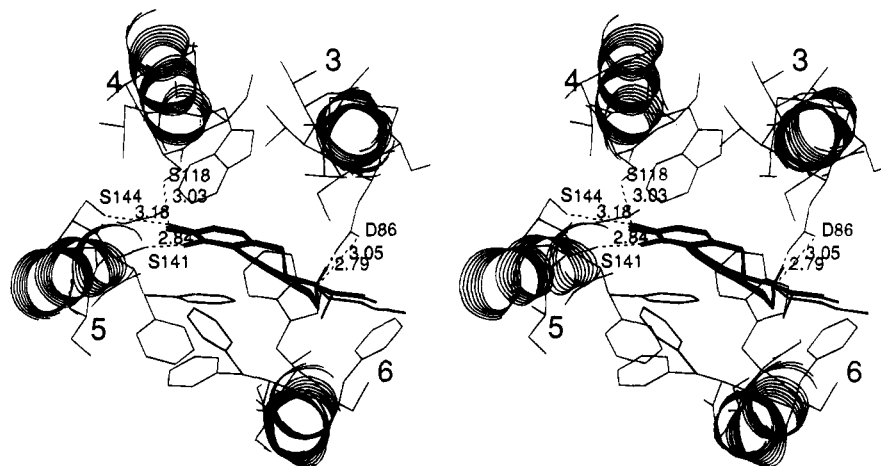


**Figure 2.** Stereoview of the dopamine binding site. The site is located between helices 3, 4, 5, and 6 which are represented by a ribbon. The docked agonists including dopamine are represented in heavy lines. The binding site is defined by Ser141 and Ser144 on the helix 5 and by Asp86 on the third transmembrane helix. The drugs were docked to be hydrogen bonded to  $O_\gamma$  of both serine residues and to  $O_{\delta 1}$  of aspartic acid and are flanked by flexible aromatic residues. Agonists fit well into the binding pocket with their least square plane perpendicular to the membrane plane.

1.5 nM is found for apomorphine and *N-n*-propylnorapomorphine (NPA), but 130–250 $\times$  weaker binding of 199–365 nM for *N-isobutyl*norapomorphine (NIBA) and *N-isopropyl*norapomorphine (NIPA).<sup>50</sup> Further, *N-n*-butyl norapomorphine (NBA) was shown to be at least 400 $\times$  less active than NPA in an *in vivo* assay.<sup>52</sup> When the other portions of agonists were well docked, the terminal carbons of NBA were too close (3.4 Å) to Thr212 backbone N (helix 7) in the extended conformation (Figure 4) and approached the  $C_{\beta s}$  of Cys181 (helix 6) and Phe211 (helix 7) as well as the S of Cys90 (helix 3) and  $C_\delta$  of Trp182 (helix 6) when rotated. The bulky isopropyl group made close contacts with the backbone of helix 6 at one methyl of the tertiary C (3.1 Å) and was close on the other side to the S of Cys90 (3.6 Å).

The *N*-methyl or *N*-phenethyl derivatives of *trans*-octahydrobenzo[*f*]quinoline are high-affinity  $D_2$  agonists where the *N*-alkyl group extends in a different direction than for apomorphine (parallel to the helix axis rather than toward it). When this compound is docked into our model, the phenyl group extends into an ancillary pocket, described below, where it can interact with other aromatic groups, for example Phe82 (helix 3) and Tyr208 (helix 7). In the present model, there are close contacts for the phenyl of phenethyl that should be better fit in future models, perhaps because all Pros in helix 7 were not changed (see Methods above). However, the *N*-phenethyl group is highly flexible and the side chains of the ancillary site should be able to accommodate themselves to it.

Docked apomorphine and its derivatives were highly constrained by van der Waals contacts with aromatic rings Trp115 (helix 4) and Phe185 (helix 6) on opposite ends of the four ring mean plane and were close to Phe82 (helix 3), Phe145 (helix 5), Trp182, and Phe186 (helix 6). In addition, the hydrogen bonds to three Ser groups (Ser118, Ser141, and Ser144) and the salt bridge of the charged nitrogen to two oxygens of Asp86 (helix 3) limit its movement. Thus the alkyl groups added have little conformational freedom to readjust within the binding pocket (Figure 5).

**The Tricyclic Antagonist Binding Site Is Chiral, and Tricyclic Antagonists Dock Parallel to the Membrane Plane.** The docking of antagonists into the binding site of the dopamine  $D_2$  receptor was initiated

with the docking of the most rigid tricyclic molecule—the 3-Br analog of cyproheptadine.<sup>28</sup> Its shape was most consistent with a binding site that had the tricyclic ring system perpendicular to the transmembrane helix axes or parallel to the membrane plane (see Figure 6 for docked loxapine). This molecule, although not clinically important as an antipsychotic, aids in establishing the folding of the tricyclic ring structure since the two different foldings can be chemically separated due to a substantial energy barrier between them.<sup>53</sup> The chirality of the active enantiomer of the cyproheptadine analog also confirmed the chirality of the receptor binding pocket. Loxapine was then docked (Figure 6), followed by octaclothepein *R* and *S*, levomepromazine, trifluoperazine, and fluphenazine.

Parameters used to characterize the antagonist pharmacophore are the fold of the tricyclic system, the distance from the center of the substituted ring to the amine nitrogen, and the orientation of the quaternary amine nitrogen.<sup>28,31</sup> All proved to be important in the docking the tricyclic antagonists. These features were most constant among all the antagonists docked (Figures 7–9).

The substituted phenyl ring of all the tricyclic drugs has a specific stacking interaction with the aromatic phenylalanine rings 145 (helix 4) and 186 (helix 6), reinforcing its importance in the pharmacophore (Figure 8). This constitutes  $\pi$ - $\pi$  aromatic ring stacking of electron poor drug rings with electron-rich phenylalanine rings, and it should be enhanced by better electron-withdrawing groups on the drugs.<sup>54</sup> Consistent with this interpretation, an increase in the electron-withdrawing power of substituents on the aromatic ring in the 2-position ( $OCH_3$  to Cl to  $CF_3$ ) increases the binding constant of the drugs.<sup>32</sup> In any position other than the 2-position, the substituent would be either exposed to lipid or would interfere with the backbone of helix 6, both of which would be destabilizing. Examination of the receptor models for antagonists vs agonists reveals that Phe145 and Phe186 move further into the pocket of accommodate the smaller size of agonists tested (Figure 2; note there are two positions for these residues).

In contrast, the unsubstituted aromatic ring in the tricyclic system can have various orientations. It ex-

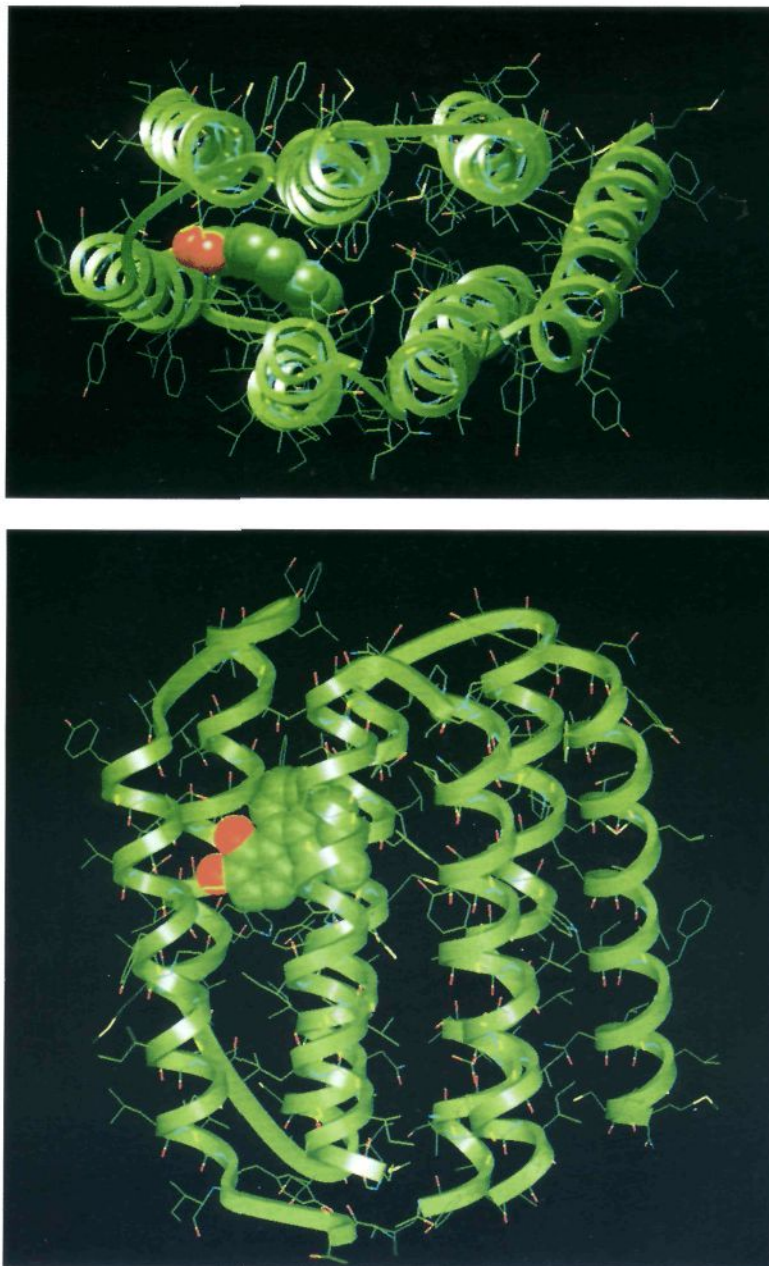


**Figure 3.** View of the dopamine D<sub>2</sub> receptor model with the agonist apomorphine docked at the binding site. The transmembrane helices are represented by solid ribbon, and the drug is in space filling representation with two binding hydroxyl oxygens in red and nitrogen (partially hidden) in blue. (a, Top) View down the helix axis. (b, Bottom) View in the plane of the helices. The extracellular space is in the upper part of the figure.

tends from the central heteroatom ring in various positions depending on the compound (Figure 9). Several positions can be accommodated in the binding site, due in part to the occurrence of Trp115 (helix 4) at the periphery of the site. Trp115 adopts one conformation ( $x_1 = -72^\circ$ ,  $x_2 = 98-129^\circ$ ) if the drug is loxapine and another conformation ( $x_1 = -77^\circ$ ,  $x_2 = 187^\circ$ ) if the drug is cyproheptadine analog. Thus the value of  $x_2$  can differ by  $90^\circ$  and still provide tight binding. Note that Trp115 takes the latter position for agonists (Figures 2 and 5).

Trp182 and Phe185 also accommodate tricyclic drugs of various shapes by adopting two conformations. For octaclothepein *R*, Trp182 has  $x_1 = -51^\circ$  and  $x_2 = 163^\circ$ , but for the rest of the antagonist drugs docked, it has  $x_1 = -61^\circ$  and  $x_2 = -11^\circ$  to  $-39^\circ$ . Phe185 has  $x_1 = -165^\circ$ ,  $x_2 = 131^\circ$  for octaclothepein *R* and  $x_1 = -152^\circ$ ,  $x_2 = 131^\circ$  for the other drugs docked.

The different activity of *N*-substituted *cis*- vs *trans*-octahydrobenzo[*l*]quinoline provides another interesting test of our model and further illustrates the role of aromatic residues. The *trans* compound is a D<sub>2</sub> agonist while the corresponding *cis* compound is only weakly active at best and may have antagonist properties.<sup>55</sup> Docking these two molecules into our active site can explain these differences. The *trans* compound is nearly planar and fits well with the agonist docking described above so that the mean plane of the rings lies perpendicular to the membrane plane and parallel to the helix axes. The *cis* compound, on the other hand, has partial agonist or mixed agonist/antagonist activity and has one ring, which contains the ammonium nitrogen, that is out of the plane.<sup>55</sup> When docked as an agonist, this ring comes close to Trp182, which forms the floor of the binding pocket as viewed in Figures 5 and 7. It may

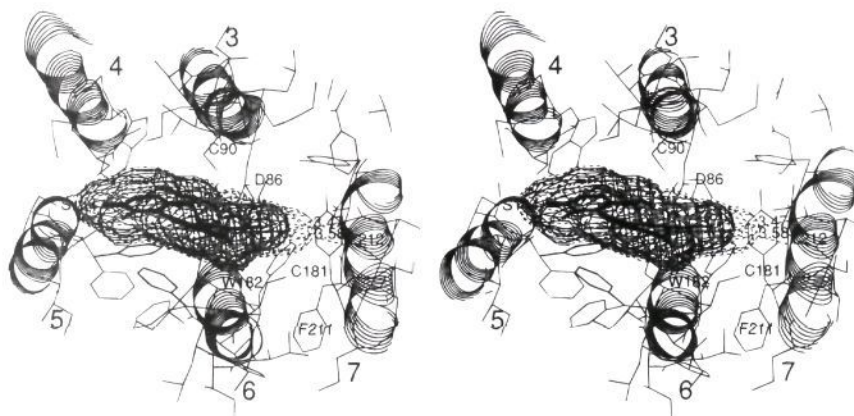


**Figure 4.** Stereoview of docked agonists covered with the space-filling Barry surface. Steric limitations imposed on the agonist size by the receptor model are shown. Note the short van der Waals contacts between methyl group of *n*-butylnorapomorphine and the backbone atoms of the helix 7. The view is the same as in Figure 2.



**Figure 5.** The binding pocket lined with aromatic residues covered with space-filling Barry surface (in orange) representation. The agonist apomorphine is shown with a space-filling Connolly dot surface (in green). Same view as in Figure 2.

dock better if the plane of the ring with the drug hydroxyls is parallel to the membrane plane, i.e., closer to the docked antagonist position. Although rotation of the compound would break a catechol hydrogen bond to a Ser144 on helix 5, a compensating hydrogen bond could be made with Ser118 on helix 4.

**Role of Aromatic Residues in Binding Pocket: Flexibility.** Analysis of the bacteriorhodopsin structure revealed that most amino acid side chains had conformations close to  $+60^\circ$ ,  $-60^\circ$ , or  $180^\circ$  except for aromatic amino acids surrounding the retinal chromophore (M. M. Teeter, unpublished results). Aromatic side chains are bulky, have low barriers for rotation, and are ideal to adjust to the changing conformation of retinal for bacteriorhodopsin throughout its proton pumping cycle or for rhodopsin in its photocycle. One might expect a similar role for these residues in G protein-coupled receptors, except that the conformation of the ligand does not change. Instead, many of these receptors have high- and low-affinity states for agonist binding in which aromatic residues might be involved (see below).

Indeed, in the dopamine receptors, the binding site proved to be lined with aromatic side chains. In this

case, such residues can adjust to the different shapes of the agonists and antagonists in the binding site. Phe185 and Trp115 border opposite sides of the binding site with their aromatic rings perpendicular to the mean ring plane of the tricyclic rings (Figure 7). The position of Phe185 is restricted by its close packing against Phe211 in helix 7, as well as by the drug. Trp182 stacks under the ring or chain with the ammonium nitrogen of the drug (Figure 7). Phe145 and Phe186 pack against the substituted ring of tricyclic antagonists and provide a wall of the binding site for agonists (Figures 8 and 2, respectively). Phe82 is also perpendicular to the tricyclic ring plane (Figure 7). Each aromatic serves a role in defining the pocket and allowing it to adjust to differently shaped molecules binding to it. Such groups could close down the site when agonist molecules bind with their smaller profile in the membrane plane and open it up to allow room for molecules larger in the plane.

**The Square Pyramidal  $\text{Na}^+$  Regulatory Site: Allosteric Regulation and Receptor Activation.** A clear path extends from the intracellular side of the cell membrane to a roughly square pyramidal region with Asp46 at one vertex between helices 2, 3, and 7 (Figure 10). Asp46 is nearly universally conserved in G protein-coupled receptors and has been shown to be involved in allosteric regulation of ligand binding by intracellular cation concentration.<sup>33–36</sup> The region near Asp46 will be referred to as the  $\text{Na}^+$  regulatory site. This sodium entry site is lined with residues which are highly conserved in the catecholamine family of receptors.

In the current model, Asp46 can change conformations between a  $x_1$  value of  $-60^\circ$  and  $+180^\circ$  without significant steric hindrance. In the former position, it points toward helix 3 and interacts with Asn96 ( $3.0 \text{ \AA}$ ). In the latter, it points toward helix 1 and interacts with Asn27 ( $\text{Asp46O}_{\delta 2}-\text{Asn27N}_{\delta 2} = 3.0 \text{ \AA}$ ) and Cys31 ( $\text{Asp46O}_{\delta 1}-\text{Cys31S}_{\gamma} = 4 \text{ \AA}$ ). Thus, there is the possibility of ionic interactions or hydrogen bonding. As Asp46 moves between  $-60^\circ$  and  $+180^\circ$ , the sodium site changes shape, but with either conformation of Asp46, the entry path or access channel is preserved.

When the  $x_1$  value of Asp46 is  $-60^\circ$ , Asp46 constitutes one vertex of a roughly square pyramidal region which could be occupied by water molecules with or without a cation, such as sodium. The base of this region is defined by Asp46 (helix 2), Asn96 and Ser93 (helix 3), and Ser219 (helix 7), whose intraresidue distances

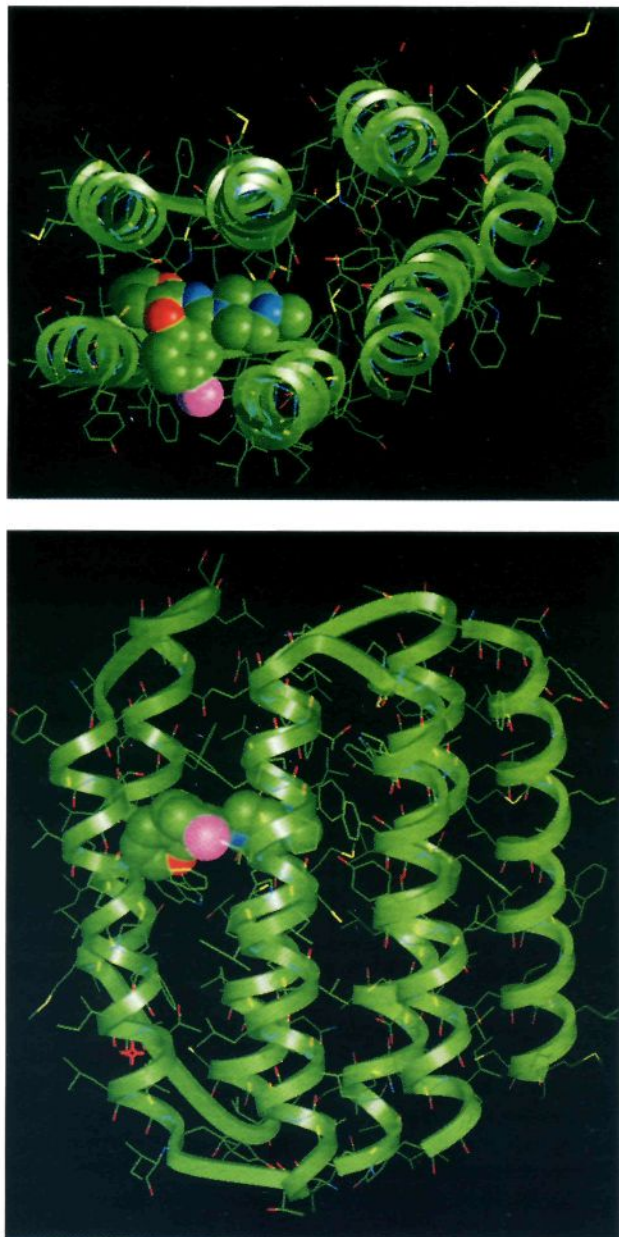


**Figure 6.** View of the dopamine D<sub>2</sub> receptor model with the antagonist loxapine docked in the binding site. Tricyclic antagonists dock with their tricyclic ring plane in the plane of the membrane. Representation as in Figure 3 except the Cl atom is in pink. (a, Top) View down the helix axes. (b, Bottom) View in the plane of the helices.

between hydrogen bonding groups vary from 4.5 to 6.0 Å. The apex is defined by Asn222. Distances from the four residues of the base to the apex at Asn222 vary between 5.9 and 8.4 Å. If Na<sup>+</sup> is at the center of this site, it can form nearly ideal interactions (Figure 10).

A positively-charged sodium ion can neutralize negative charge in this region. Ser and Asn are well suited to line such an internal Na<sup>+</sup>/water site. They can be available to bond to polar groups such as water to ions or to nearby residues or they can be held in reserve, as it were, by hydrogen bonding to the helical backbone.

**Ancillary Binding Pocket.** The space for the proposed sodium site, between helices 2, 3, and 7, could provide an extended binding pocket for drugs larger than the small tricyclic D<sub>2</sub> antagonists (see space to the right of the ligand pocket in Figures 3a and 6a). Tyr216, which corresponds to the Lys216 that forms a covalent



**Figure 7.** The group of antagonists idocked into the same binding site. Complementarity between the Connolly dot surface (in green) which cover antagonists and the Barry surface (in red) of aromatic residues forming the binding pocket can be observed. Please note a different mode of binding in which antagonists are directed perpendicular to the direction of the helices. The binding pocket floor is formed by Trp 182. Two phenylalanine rings Phe145 and Phe186 sandwich the halogen-substituted rings of antagonists at the periphery of the site.

Schiff's base link to retinal in bacteriorhodopsin, is in this pocket as well as Trp56, Met89, Tyr208, and Thr212. Risperidone is an example of a larger D<sub>2</sub> antagonist that could extend into this region and influence the sodium site and signal transduction more directly. In fact, risperidone has approximately the same length as retinal in bacteriorhodopsin, which suggests that it could occupy both portions of the binding pocket.

The large tricyclic drug fluphenazine has a piperazine ring with an N-substituted ethyl alcohol which extends into this site. The addition of the ethyl alcohol to trifluoperazine to make fluphenazine increases in binding 2–4 times, depending on the receptor state. The phenethyl substituent on N-substituted *cis*- or *trans*-octahydrobenzo[*f*]quinoline also binds in this pocket and enhances the binding. As mentioned above, this pocket is at present too tight, and future models will be adjusted to accommodate such substituents.

Substituted benzamides behave differently from tricyclic antagonists.<sup>141,34,56</sup> Binding of substituted benzamides is Na<sup>+</sup> sensitive while that of tricyclics is not. These benzamides may also dock in this secondary binding region which is contiguous with the sodium allosteric site around Asp46 (see Na<sup>+</sup> site).

**Conserved Aliphatic Residues Contribute to Stabilizing Interactions: the Aliphatic Floor.** In the proposed model, aliphatic residues that are highly conserved or homologous in catecholamine receptors are in van der Waals contact. These include Ile or Val28 (Ile/Val28), Val30 and Ile/Cys31 on helix 1; Leu42, Ala43, and Ile/Leu47 on helix 2; Ile94, Leu97, and Ile100 on helix 3; Ile/Val111 on helix 4; Tyr156 on helix 5; Leu/Val171 and Phe178 on helix 6; and Ile/Val224 on helix 7.



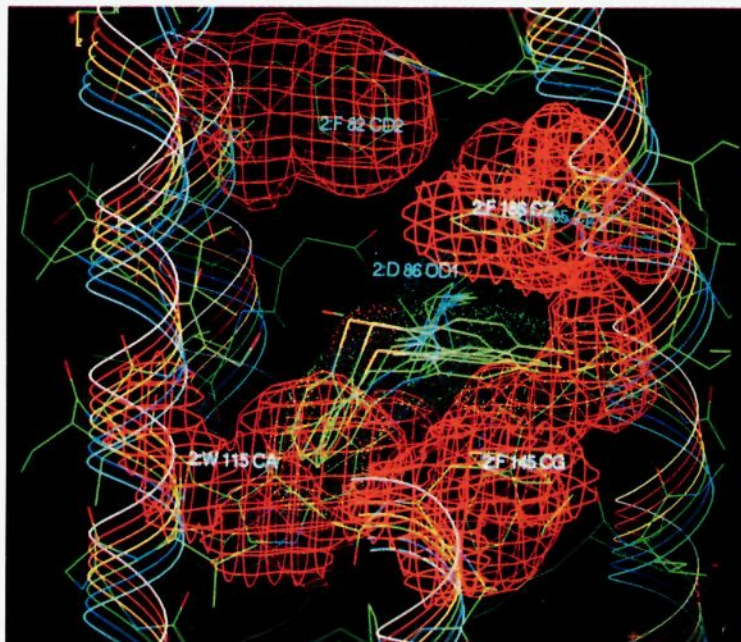


**Figure 8.** View of  $\pi$ - $\pi$  stacking of substituted tricyclic antagonist ring with aromatic Phe145 and Phe186 of the receptor in the plane of the helical axes. The antagonists loxapine, octaclothepin *R* and *S* and levomepromazine are covered with a composite Connolly dot surface. Aromatic residues in the binding pocket have Barry surfaces and ribbons indicate the helices.

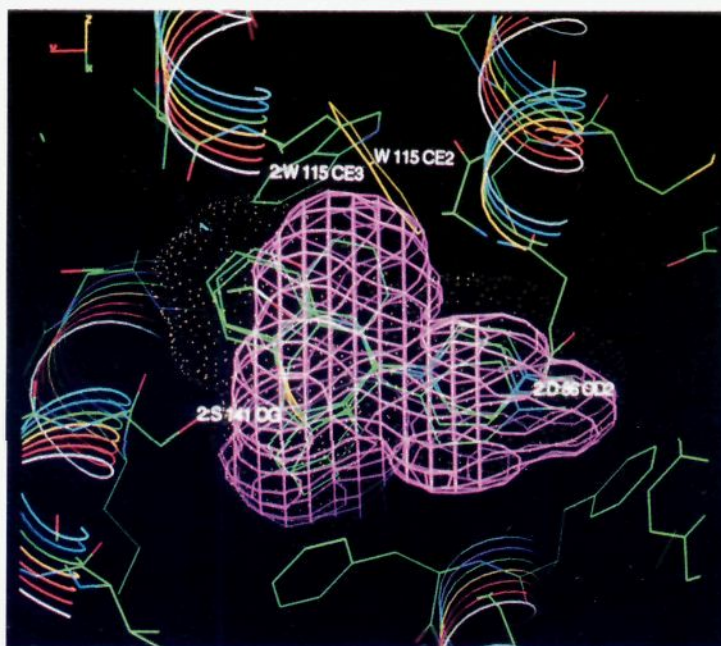


**Figure 9.** The flexibility of the binding site exemplified by the torsional adjustments of the Trp115 indole ring when different antagonists are docked. Depending on the structure of antagonist the Trp115 changes the  $\chi_2$  conformation from  $\sim 180^\circ$  to  $\sim 90^\circ$  to accommodate different ring organization of the drugs. The yellow dot surface for antagonists correlates with the yellow Trp115 conformation and the purple Barry surface of cyproheptadine with the other Trp conformation.

The van der Waals interactions for Ile/Cys31–Ala43, Val30–Ile/Val224, Leu42–Ile100, and Tyr156–Leu/Val171 form a plane near the cytoplasmic site of the receptor. These contacts stabilize conserved packing interactions for helices 1–2, 1–7, 2–3, and 5–6. A second stabilizing contact for helix 1 to 2, Ile/Val28–Leu47, lies 1 turn to the extracellular side of Cys/Ile31–Ala43.

The remaining conserved aliphatic interactions for Ile94–Ile/Val111 (helix 3 to 4) and Leu97–Phe178 (helix 3 to 6) lie on the cytoplasmic side of Trp115. They stabilize the primary ligand binding site.

Where residues are homologous (indicated by a slash) rather than conserved, the atoms in contact remain the

same, despite the residue's identity. Aliphatic residues conserved are for catecholamine receptors primarily. Exceptions are Leu42 and Ala43, which are more widely conserved.

**Summary of Results.** Presented here is a data-based model for the dopamine  $D_2$  receptor from the coordinates of bacteriorhodopsin. The testing of this model with semirigid agonists and antagonists brings to light different modes of binding for agonists and antagonists: parallel vs perpendicular to the membrane plane respectively (Figures 3 and 6). These differences could have important implications for conformational changes between high- and low-affinity states and mechanisms of signal transduction.

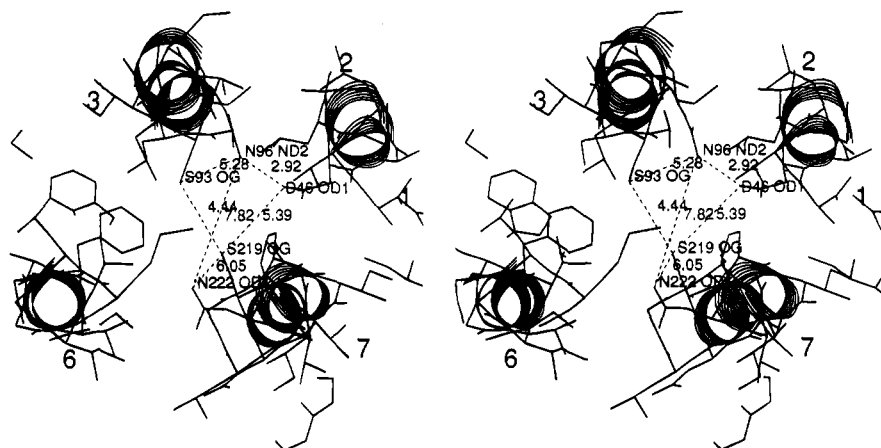


**Figure 10.** Stereoview of the proposed sodium binding site. It is located close to the cytoplasmic end of the receptor between transmembrane helices 2, 3, and 7. Roughly square pyramidal coordination of the site is formed by the O<sub>γ</sub> of Ser93 and Ser219, and side chain oxygens of Asp46, Asn96, and Asn222.

The model can account for a great deal of the structure–activity relationships of D<sub>2</sub> agonists. The loss of agonist activity that occurs for the *N*-butyl (or larger) analog of apomorphine can be seen to be due to the projection of the *N*-alkyl group toward the backbone of helix 7, which is resistant to conformational change. In contrast, the *N*-alkyl group of octahydrobenzo[*f*]quinoline which can be as large as *N*-phenethyl projects in the direction of other side chains and along the helix axes. It can be readily accommodated. Also, the agonist site favors a fairly planar ligand (apomorphine and *trans*-octahydrobenzo[*f*]quinoline, due to interactions with Trp182 at the floor of the binding site. Agonist activity is diminished for *cis*-octahydrobenzo[*f*]quinoline, where the piperidine ring projects above the plane of the molecule.

For antagonists, the model accounts for the chirality of the rigid tricyclic structure since the binding site has a complementary chirality due to the presence of aromatic side chains. The necessity of an electron-withdrawing group such as 2-Cl or 2-CF<sub>3</sub> can be understood as enhancing the stacking interactions with adjacent aromatic rings. The necessity of a heteroatom in the central ring of tricyclic antagonists can be understood since this atom can hydrogen bond with the hydroxyl of Ser141 and/or Ser118.

This D<sub>2</sub> receptor model is further supported by its explanation of three other features: allosteric Na<sup>+</sup> effects, binding of large ligands sensitive to Na<sup>+</sup> and conserved packing interactions. The Na<sup>+</sup> site (Figure 10) is located adjacent to the tricyclic binding pocket where the highly conserved Asp46 is found, a residue known to be involved in binding regulation by cations. This site is lined with Ser and Asn residues which can bond to water, to a Na<sup>+</sup> ion, or to the backbone. The ancillary binding pocket which large ligands could occupy is directly adjacent to this Na<sup>+</sup> site. Some ligands that could bind are known to be influenced by Na<sup>+</sup>. Finally, conserved aliphatic helix packing interactions stabilize the model and suggest this helix arrangement would be found for the catecholamine family. Note the absence of helix 6 to 7 interactions, which may relate to the low- and high-affinity states of the receptor (see below).

## Discussion

**An Overview.** Many residues found to be functionally important for bacteriorhodopsin are involved in

function for dopamine receptors as well. This includes the binding pocket and the cation-sensitive site. Although use of bacteriorhodopsin coordinates assured some similarity, few residues in these functionally important regions are conserved between these two molecules.

Considerable mutagenesis data strongly support the model of the binding site, the ancillary site, and the sodium site presented here. Other residues predicted to be important have no such data available. These would be good candidates for future mutagenesis study. The activation of the receptor from low- to high-affinity states is discussed in light of helix movements and specific residues that could be involved.

The model presented here shares most similarity in the main ligand binding site to that presented by Trumpp-Kallmeyer *et al.*<sup>21</sup> Differences are found in certain important residues in the primary binding site and particularly the ancillary site. However, the overall aromatic character of the site is the same. The model here is compared to others most relevant. No one has previously noted a Na<sup>+</sup> binding site for these G protein coupled receptors.

Helical wheel analysis of conservation in G protein coupled receptors has been used by Baldwin<sup>57</sup> to interpret the two-dimensional projection data for rhodopsin transmembrane helices presented by Schertler.<sup>37</sup> Baldwin's objections to the use of the bacteriorhodopsin helical arrangement are answered in the presented model. Although the projection of rhodopsin does differ from the projection of bacteriorhodopsin, i.e., one helix has moved out, the two receptors may be in different states (11- or 13-*cis* vs *trans* bond for retinal). Schertler does not provide data about the receptor state.<sup>37</sup>

**Comparison of Bacteriorhodopsin Retinal Binding Site, Proton Channel, and Na<sup>+</sup> Site/Binding Pocket.** Many of the residues important for binding retinal are those involved in ligand binding and Na<sup>+</sup> regulation for the dopamine receptors, and by analogy, for the G protein-coupled receptors. Retinal extends along the interior of the packed bacteriorhodopsin helices with its ring at the tricyclic binding pocket and its unsaturated tail in the ancillary pocket. The Schiff base attachment of retinal (Lys216) is near the proposed Na<sup>+</sup> site and the ancillary site where larger drugs such as spiperone and haloperidol bind.

Table 2 presents a comparison of important residues in the model presented here with those in bacterio-

rhodopsin in its trans retinal binding site and its proton channel. For most of the residues, there is a direct correspondence. Thus, just as there is a weak sequence homology but a similar fold of the two proteins, so there appears to be a strong homology in overall structure and functionally important residues. Further, comparison of the D<sub>2</sub> model presented here with that of bacteriorhodopsin reveals a common region for binding of tricyclic ligands from outside the cell, a common region for the entry of intracellular cations, and a connection between these two regions, which in bacteriorhodopsin is occupied by retinal.<sup>2,15</sup>

**Mutagenesis Studies and How Our Model Was Found To Be Compatible with This Data.** We have examined a number of mutagenesis studies of dopamine and related receptors in a further effort to evaluate the D<sub>2</sub> model. This discussion is divided into five parts: ligand binding residues, other binding pocket residues, ancillary pocket and entry residues, sodium site residues, and other residues.

In the primary tricyclic binding pocket for the model presented here are the ligand binding residues Asp86, Ser141, and Ser144 as well as residues Phe82, Cys90, Trp115, Ser118, Ser122, Phe145, Trp182, Phe185, and Phe186 (Figures 2, 4, and 7–9). Of these residues, no published data was found for Phe82 on helix 3 and for Trp115, Ser118, or Ser122 on helix 4 for any of the G protein-coupled receptors. The ancillary pocket contains Trp56, Met89, Tyr208, Thr212, and Tyr216. No mutagenesis data was found for Trp56 or Tyr208.

**The Three Ligand Binding Residues.** Asp86 (helix 3) is a highly conserved residue which has been studied in D<sub>1</sub>,<sup>57</sup> D<sub>2</sub>,<sup>58,59</sup> and a number of other G protein-coupled receptors, including rhodopsin,<sup>5</sup>  $\beta$ -adrenergic,<sup>11,60</sup>  $\alpha_2$ -adrenergic,<sup>61</sup> 5HT<sub>2</sub>,<sup>62</sup> and a muscarinic receptor.<sup>21</sup> Each study of mutation of this residue supported its importance as the binding site for the ammonium nitrogen of agonists and antagonists. Mutations resulted in marked reduction of ligand binding.

There is strong evidence that Ser141 and Ser144 (helix 5) are hydrogen-bonding sites for the *m*- and *p*-OH of epinephrine and dopamine (Figure 2). Mutations of these residues have been studied in D<sub>1</sub>,<sup>57,63</sup> D<sub>2</sub>,<sup>58</sup>  $\beta$ -adrenergic receptors,<sup>12,63</sup> and, for Ser144, in  $\alpha_2$ -adrenergic receptors.<sup>61</sup> For D<sub>2</sub> receptors, there is evidence from the Ala mutants that Ser144 is more important than Ser141 for dopamine binding.<sup>58</sup> Since the authors thought that the *m*-OH of dopamine is more important, they concluded that the *m*-OH bonds to Ser144, which would be different from the pattern of epinephrine bonding to  $\beta$ -adrenergic receptor. The modeling presented here is more consistent with the  $\beta$ -adrenergic pattern and suggests both OH groups are important for dopamine binding.

**Other Binding Pocket Residues.** Trp182, Phe185, and Phe186 (helix 6) are in the highly conserved sequence CWLPFF. In rhodopsin<sup>64</sup> and muscarinic (M<sub>3</sub>) receptors,<sup>65</sup> Trp182 showed decreased affinity and lower activation of the G protein, suggesting that Trp182 is an important element in ligand binding as well as in the mechanism of signal transduction (Figures 5 and 7). The fact that Phe185 mutants resulted in reduction of signal transduction suggests that it is also a functional element in the mechanism.<sup>21,58,65–67</sup> Several studies of Phe186<sup>5,21,66,67</sup> done with the homologous

residues in D<sub>2</sub>, 5HT<sub>2</sub>,  $\beta$ -adrenergic, and muscarinic receptors show direct involvement of Phe186 with drug binding (Figure 8). The D<sub>2</sub> mutants with Ala for Phe186 had no affinity for either agonists or antagonists, although the receptor was expressed and inserted in the membrane. In the muscarinic receptor study,<sup>5</sup> Phe186 was found to interact with the ester of acetylcholine. The 5HT<sub>2</sub> study was consistent with Phe186 serving to anchor serotonin in the binding pocket. That study also found Phe186 to be important for generation of the second messenger, which suggests a role for Phe186 in receptor activation.

**Ancillary Binding Pocket Residues.** Met 89 was studied in D<sub>1</sub><sup>57</sup> and D<sub>2</sub><sup>58</sup> receptors. In a study of D<sub>1</sub> receptors, Cys89 and Ser90 were mutated to A and G, respectively (Figure 5).<sup>57</sup> A decrease in agonist and antagonist affinity suggested to authors that these residues may participate in the ligand binding site. In D<sub>2</sub> receptors mutation of Phe145 (helix 5) to Ala was associated with an increase in K<sub>d</sub> for spiperone and raclopride, again supporting its presence in the binding site (Figure 8).<sup>58</sup>

Thr212 (helix 7) is conserved in D<sub>2</sub>, D<sub>3</sub>, and D<sub>4</sub> dopamine receptors but is Val in D<sub>1</sub> and D<sub>5</sub>. In the presented model, Thr212 is in the ancillary binding pocket and can interact with Asp86 (Figure 4). Mutagenesis studies in 5HT<sub>1a</sub>, 5HT<sub>1b</sub>,  $\alpha_2$ -adrenergic,  $\beta$ -adrenergic, and M3 demonstrate the corresponding residue to be important in ligand affinity.<sup>65,68–70</sup> In fact, in the human 5HT<sub>1b</sub> receptor the mutagenesis of the corresponding residue (which is also Thr) to Asn changed the pharmacology of the receptor to that of the rodent sequence, which contains Asn at residue 212. This demonstrates the critical importance of 212 to the binding of ligands to the 5HT<sub>1b</sub> receptor and its likely location in the binding pocket.

Tyr216, which corresponds to the site of Lys216-retinal Schiff base in bacteriorhodopsin and rhodopsin, has been studied in D<sub>1</sub>, D<sub>2</sub>, and M<sub>3</sub> receptors. Chemical modification and pH studies<sup>20</sup> implicate this residue in ligand binding and thus support models which include it in the ligand-binding region. In D<sub>1</sub>, where 216 is a Trp, mutation to Tyr results in decreased antagonist affinity, but no change in dopamine affinity, which suggested to the authors<sup>57</sup> that 216 interacts only with antagonists (Figures 2–4).

**Sodium Site Residues.** The residues important in the sodium binding site include Asn27, Cys31 (helix 1), Asp46 (helix 2), Ser 93, Asp96 (helix 3), Asn218, Ser219, Asn222 (helix 7) as well as indirect effects from Cys181 (Figure 10). We could find no published mutagenesis data on residues Asn27, Cys31, Ser93, and Asn96. Residues which define the base and apex of the square pyramid are conserved in many or most G protein-coupled receptors. These include Ser93 and Asn96 in helix 3 (conserved in many); Ser219 and Asn222 in helix 7 (conserved in most); and Asp46 in helix 1 (conserved in virtually all). Mutagenesis here affected not only ligand binding but second messenger activity.

There are mutagenesis studies for Asp46 for D<sub>2</sub>,<sup>5,34</sup>  $\alpha_2$ -adrenergic,<sup>35,61</sup>  $\beta$ -adrenergic,<sup>11,60,71</sup> D<sub>1</sub>,<sup>57</sup> S<sub>1a</sub>,<sup>72</sup> S<sub>2</sub>,<sup>62</sup> and gonadotropin-releasing hormone<sup>73</sup> receptors. These studies show that Asp46 is important for agonist binding, G protein activation, and allosteric regulation of coupling by cations, i.e., increased K<sub>d</sub> for agonists and

decreased  $K_d$  or no change in  $K_d$  for antagonists, decrease in  $K_{diss,GDP}$ , and decrease in  $K_{act}$  for the effector enzyme.

Mutations in Asn218, Ser219, and Asn222 all increased the  $K_d$ s of agonists.<sup>60,67,72</sup> Change of residue Asn218 to Lys in  $\beta$ -adrenergic receptors resulted in no change in antagonist  $K_d$ .<sup>60</sup> Mutation of Asn222 to Ala, Phe, or Val in 5HT<sub>1a</sub> receptors demonstrated no agonist affinity.<sup>72</sup> However, when this residue was changed to Gln, there was no effect on agonist affinity. Gln would preserve the hydrogen bonding character of Asn while the other changes would not.

**Other Important Residues.** Thr168, located at the juncture of the third intracytoplasmic loop and the start of helix 6, corresponds to Ala in  $\alpha_{1b}$ -adrenergic receptors. Mutation of this residue from Ala to any other residue resulted in constitutive activation of the receptors.<sup>74</sup> Receptors displayed a graded elevation of G protein coupling in the absence of agonist, and all mutants demonstrated higher affinity for agonists, suggesting that this part of the receptor may serve to constrain G protein coupling and further, that this restraint is relieved by agonist binding. In the D<sub>2</sub> model, the next residue, Gln169, can interact with Asn222 in helix 7. It is possible that this bond cannot form in constitutively active mutants in which residue 168 has been replaced by anything else. Thus, in D<sub>2</sub>, residue 169 could form a restricting bond with helix 7 which is broken during receptor activation.

In the  $\beta$ -adrenergic receptor the Cys181 (helix 6) to Ser mutant<sup>75</sup> had normal ligand binding but attenuated ability to mediate stimulation of adenylate cyclase, suggesting to the author that Cys181 may assist in maintaining the receptor conformation required for interaction with and activation of G<sub>s</sub> (Figure 4). In a study of D<sub>1</sub> receptors,<sup>58</sup> the Cys181 to Val mutant was found to have a doubling of  $K_d$  for both agonists and antagonists, which suggests that it could be active in mechanisms of receptor function. Further, Cys181 may be involved in the mechanism of signal transduction, according to results of a study of this conserved residue in  $\beta$ -adrenergic receptors.<sup>75</sup> It is noteworthy that the D<sub>2</sub> model suggests a potential interaction between Cys181 and Asn218 in one conformational state.

His189 is a residue on helix 6 which lines the entry site for the primary ligand binding pocket in the model presented here (Figure 7). It is conserved in D<sub>2</sub>, D<sub>3</sub> and D<sub>4</sub> dopamine receptors but is Asn in D<sub>1</sub> and D<sub>5</sub>. His189 was implicated in ligand binding<sup>20</sup> and was important in specification of antagonist affinity,<sup>67</sup> which again is supportive of our D<sub>2</sub> model.

**Candidates for Future Mutagenesis Studies of D<sub>2</sub> Receptors.** Among the residues for which no mutagenesis data is available, the ones most important in the presented model are Trp115 and Ser118 in the ligand pocket and Asn27, Ser93, and Asn96 in the allosteric Na<sup>+</sup> site. Trp115 forms an important wall of the ligand site (Figure 9), and Ser118 adds hydrogen bonds to stabilize certain ligands (Figure 2). No mutations have been done for helix 1 and Asn27 on this helix could be important in providing stabilization for Asp46. Ser93 and Asn96 are important components of the square pyramidal Na<sup>+</sup> binding site (Figure 10).

**High- and Low-Affinity Receptor States and Receptor Activation.** Dopamine D<sub>2</sub> receptors have high- and low-affinity states for agonists,<sup>76</sup> but antago-

nist have a single state. The effect of mutants on the binding of agonists may be due to the change in receptor from high- to low-affinity states. The high-affinity state may be needed for receptors to activate G proteins, although the link is not completely clear.

The fact that Na<sup>+</sup> and mutations that change Na<sup>+</sup> binding decrease the binding of agonists may be due to destabilization of the high-affinity state. This in turn might result in reduced receptor activation.

Thr212 and Tyr216 are close enough to Asp86 to weakly hydrogen bond to it. Na<sup>+</sup> binding might weaken these interactions and could in turn alter their influence on Asp86 in such a way as to decrease affinity for agonists and to release helix 7. This might also contribute to the differences between the high- and low-affinity states of dopamine receptors.

Certain residues were noted above to have an effect on receptor activation. These include Phe185, Phe186, and Trp182 in the ligand binding pocket, Asp46 in the Na<sup>+</sup> site, and Cys181 and Thr168 as other important residues.

On the basis of mutagenesis data presented that implicate change in state of the receptor or receptor activation and the few interactions in the current model for helix 7, we hypothesize that helix 7 could move between the high- and low-affinity states of the receptor and thus influence receptor activation.<sup>53</sup> Several residues that affect receptor activation interact with helix 7: Phe185 (Figure 5) stacks with Tyr208 and Asp46 is involved in Na<sup>+</sup> site binding with residues Ser219 and Asn222 (Figure 10).

In the model presented here, helix 7 is the only helix which has few bonding interactions with adjacent helices and the only helix which is parallel to an adjacent helix (helix 1). No conserved aliphatic floor contacts are formed for helix 6 and 7. Further, helix 7 forms a loop with only one adjacent helix. This could allow more freedom of lateral movement in the membrane plane. Yet, if helix 7 were closer to adjacent helices it could be held by specific bonding interactions. These include Cys181 and Gln169 (helix 6) to Asn218 and Asn222 (helix 7), and Ser219 (helix 7) to Ser93, Ser96 (helix 3), or Asp46 (the Na<sup>+</sup> site on helix 2).

**Comparison with Certain Other Models That Have Been Built.** Hibert *et al.*<sup>19</sup> and Trump-Kallmeyer *et al.*<sup>21</sup> built models based on homologies in 24 and later 39 G protein-coupled receptors and examined D<sub>2</sub> receptors and others in some detail. Their methodology is similar to our own except for their important decision to use ideal helices and a different alignment with bacteriorhodopsin from the one presented here in transmembrane regions 3 and 4. In addition, their alignment with bacteriorhodopsin differs from the 1992 and 1991 papers. The basis for their primary alignment and the reason for the change of alignment in helices 1, 3, 4, and 5 between the two papers is unclear. Sequence alignment with bacteriorhodopsin is critical for any model.

The D<sub>2</sub> model presented here defines a binding pocket with important differences from that of Trump-Kallmeyer *et al.*<sup>21</sup> These differences are supported by the mutagenesis studies summarized above. Our model defines Cys90 (helix 3) as an additional binding pocket residue and reveals an extension from the main pocket into an ancillary binding pocket which contains Thr212 and Tyr216 (helix 7). There are numerous mutagenesis

studies which support these residues being important in ligand binding, as discussed above. Further, Tyr146 in helix 5 and Phe178 in helix 6 Trumpp-Kallmeyer *et al.*<sup>21</sup> model were not in the binding pocket between our model, and neither residue has mutagenesis data available. For the binding pocket residues which are common in our model and that of Trumpp-Kallmeyer *et al.*,<sup>21</sup> mutagenesis studies support these residues being in the pocket.

Zhang and Weinstein<sup>22</sup> proposed a different order of helices and helix-helix packing based on individual homology of the transmembrane regions to bacteriorhodopsin. When the method described here is applied to their proposed alignment, the resultant model does not dock substrates well. Whether this indicates a limit of our method or genuine differences will have to await mutagenesis studies to distinguish the two models. A recent model for the gonadotropin-releasing hormone receptor<sup>73</sup> on which Weinstein was an author shows the same helix packing as our model.

Livingstone<sup>20,77</sup> used a different alignment with bacteriorhodopsin for three of the D<sub>2</sub> helices (1, 4, and 5). The resulting model of D<sub>2</sub>-like dopamine receptors was built with idealized helices which were superimposed on bacteriorhodopsin helices. Livingstone also noted that homology matching of primary sequences resulted in several regions being inconsistent with biochemical and mutational data, which required their realignment of those helical regions.

We examined the Livingstone alignment with our model but we could not confirm their observations. This suggests that their C<sub>α</sub> chain coordinates differed significantly from the actual bacteriorhodopsin coordinates which we used. For example, dopamine docking was not possible with Asp86, Ser141, and Ser144 since distances were inappropriate for bonding. Livingstone reported parallel stacking between dopamine and Trp182, between the thiophene ring of N-0437 and Tyr216, and between Tyr216 and Trp82, none of which agree with the model presented.

Livingstone contrasted their model with that of Hibert *et al.*<sup>19</sup> They note that Hibert found Phe145 and Phe186 to stack with the catechol ring of dopamine, which Livingstone could not confirm because distances between them were too great. In the presented model, the catechol ring of dopamine is constrained by hydrogen bonds to Ser141 and Ser144 for the *m*- and *p*-OH (Figures 2 and 3a). It appears that these differences were based on different primary sequence alignments in the two models.

Baldwin<sup>66</sup> suggested differences between the rhodopsin projection data<sup>37</sup> and the known two-dimensional arrangement of helices in the bacteriorhodopsin structure based on her analysis. She had examined structural implications of conservation and variation of amino acids in 204 G protein-coupled receptor sequences and proposed a three-dimensional arrangement of the helices of G protein-coupled receptors from this analysis via helical wheels as compared to the recent low-resolution projection map of rhodopsin.<sup>37</sup> Differences with bacteriorhodopsin were based on two considerations: disulfide bridge formation between helix 3 and the extracellular loop before helix 5<sup>13,78,79</sup> and the apparent location of ligand binding residues.

First, Baldwin observed that, in D<sub>2</sub> and 5-HT<sub>2</sub> receptors, there are only five residues between the second

Cys and the beginning of helix 5 (in bacteriorhodopsin there is no such constraint and no Cys in those loops). Formation of disulfide bridge in D<sub>2</sub> and 5-HT<sub>2</sub> receptors requires the extracellular portions of helices 3 and 5 to be closer together than is the case in bacteriorhodopsin, based on helical wheels.

Secondly, from other studies of residues binding to epinephrine acetylcholine,<sup>12,60,63,79-81</sup> it appeared that positioning the helical wheels on the bacteriorhodopsin helices would not allow appropriate binding for these short ligands.

After altering the helical wheel arrangement so that docking of small ligands appeared appropriate and the disulfide bond between the Cys residues near the beginning of helices 3 and 5 appeared plausible, the proposed arrangement of the helical wheel model was compared with electron diffraction derived projections of bacteriorhodopsin and rhodopsin two-dimensional crystals. Baldwin's comparison clearly favored the rhodopsin projection structure,<sup>37</sup> although tacit assumptions were made that both molecules were studied in equivalent states.

When Baldwin's helical wheels of the D<sub>2</sub> receptor are compared with those presented for the model described in this paper, the alignment is identical, with only minor adjustments. However, when the actual bacteriorhodopsin coordinates are used to generate the tertiary structure, limitations of helical wheels become apparent. The three-dimensional model presented here does not seem to suffer from the limitations proposed in the Baldwin paper.

The helical wheel for helix 5 shows Ser141 and Ser144 unavailable for bonding to small agonist ligands (Figure 1b). However, the actual bacteriorhodopsin coordinates resulted in small differences in location of residues and docking to the three-dimensional model was obvious with excellent bonding distances and angles, as discussed above (Figures 2). Based on variation from ideal angles in the bacteriorhodopsin coordinates, these two residues are directly over one another in the D<sub>2</sub> model viewed down the helix axes, rather than 60° apart as suggested by Baldwin from the helical wheel diagram. The actual position of these C<sub>α</sub>'s results in the vertical docking of agonists as discussed above. This observation could not have been made if our model had been based on theoretical, helical wheel considerations.

Baldwin's suggestion that formation of an extracellular disulfide bridge between two highly conserved Cys residues is impossible with bacteriorhodopsin helical wheels was examined in the presented model. In the short loop between helices 4 and 5 in D<sub>2</sub>, there appears to be enough available space for such a bridge. Thus, no problems were encountered in forming this disulfide from a model based on bacteriorhodopsin.

The question remains as to the difference between the rhodopsin and bacteriorhodopsin projections<sup>37</sup> in relation to the model presented here. The rhodopsin and bacteriorhodopsin receptors may have been studied in different conformations and thus have different helical dispositions (corresponding to high vs low affinity or activated vs inactivated receptor). The retinal conformation is not specified in the article. Thus, the fact that the model proposed in this paper agrees more with the bacteriorhodopsin projections may or may not be in disagreement with the rhodopsin projection. Others<sup>82</sup> suggest that slightly tilted helices could result in

radically different projection data. More data on receptor state and a higher resolution diffraction pattern for rhodopsin crystals is needed to make this distinction.

### Conclusions

It can be seen from the mutagenesis data that there is substantial support for the model which has been proposed here. All the residues in common between the Trumpp-Kallmeyer *et al.* model<sup>21</sup> and the one presented here are substantiated by mutagenesis. In addition, residues Met89, Cys90, His189, and Thr212 are identified by mutagenesis to be important but are not in the Trumpp-Kallmeyer *et al.* model. Several residues suggested to be important in Na<sup>+</sup> regulation have no mutagenesis data at present.

Further mutagenesis must be done to distinguish the model presented here from other models presented and to provide a firmer basis for drug design. However, using semirigid agonists and tricyclic antagonists, it has been possible to define much of the stereochemistry of the model and construct a model that rationalizes much of the drug data currently available on D<sub>2</sub> dopamine receptors.

Finally, this model suggests an alternate interpretation of the recent rhodopsin projection structure. Observations on rhodopsin and bacteriorhodopsin could have been made with these receptors in different but interconverting conformational states or with a different helical tilt.

Future research in this area should expand the understanding of high- and low-affinity state for D<sub>2</sub> receptors as well as mechanisms of coupling to G proteins. A recent crystal structure of transducin- $\alpha$ ,<sup>83</sup> the G protein linked to rhodopsin, should aid this analysis.

**Acknowledgment.** The authors wish to thank the NIH for Grant R01 GM38114 for support for homology modeling to M.M.T. and for a postdoctoral fellowship (B.S.) and the National Institute on Drug Abuse for Grant DA 06681 to M.F. We also wish to thank Richard Deth for helpful discussions.

### References

- Hartig, P. Slow transmitter G protein coupled receptors: the 5HT superfamily as drug targets. *Am. Col. Neuropsychopharm.* **1993**, *14*.
- Henderson, R.; Schertler, G. F. X. The structure of bacteriorhodopsin and its relevance to the visual opsins and other seven-helix G-protein coupled receptors. *Phil. Trans. R. Soc. London* **1990**, *326*, 379–389.
- O'Dowd, B. F.; Nguyen, T.; Tirpak, A.; Jarvie, K. R.; Israel, Y.; Seeman, P.; Niznik, H. B. Cloning of two additional catecholamine receptors from rat brain. *FEBS* **1990**, *262*, 8–12.
- Venter, J. C.; Fraser, C.; Kerlavage, A.; Buck, M. L. Molecular biology of adrenergic and muscarinic receptors. *Biochem. Pharmacol.* **1989**, *38*, 1197–1208.
- Probst, W. C.; Snyder, L. A.; Schuster, D. I.; Brosius, J.; Sealfon, S. C. Sequence Alignment of the G-Protein Coupled Receptor Superfamily. *DNA Cell Biol.* **1992**, *11*, 1–20.
- Birnbaumer, L. G proteins in signal transduction. *Annu. Rev. Pharmacol. Toxicol.* **1990**, *30*, 675–705.
- Seeman, P. Dopamine receptors and the dopamine hypothesis of schizophrenia. *Synapse* **1987**, *1*, 1333–152.
- Seeman, P.; Niznik, H. B.; Guan, H.-C.; Booth, G.; Ulpian, A. C. Link between D1 and D2 dopamine receptors is reduced in schizophrenia and Huntington diseased brain. *PNAS* **1989**, *86*, 10156–10160.
- Dixon, R. A. F.; Kobilka, B. K.; Strader, D. J.; Benovic, J. L.; Dohlman, H. G.; Frielle, T.; Bolanowski, M. A.; Bennett, C. D.; Rands, E.; Diehl, R. E.; Mumford, R. A.; Slater, E. E.; Sigal, I. S.; Caron, M. G.; Lefkowitz, R. J.; Strader, C. D. Cloning of the gene and cDNA for mammalian beta-adrenergic receptor and homology with rhodopsin. *Nature* **1986**, *321*, 75–79.
- O'Dowd, B. F.; Hnatowish, M.; Caron, M. G.; Lefkowitz, R. J.; Bouvier, M. Palmitoylation of the human beta2-adrenergic receptor. *J. Biol. Chem.* **1989**, *264*, 7564–7569.
- Strader, C. D.; Sigal, I. S.; Candelore, M. R.; Rands, E.; Hill, W. S.; Dixon, R. A. F. Conserved aspartic acid residues 79 and 113 of the beta-adrenergic receptor have different roles in receptor function. *J. Biol. Chem.* **1988**, *263*, 10267–10271.
- Strader, C.; Candelore, M. R.; Hill, W. S.; Sigal, I. S.; Dixon, R. A. F. Identification of two serine residues involved in agonist activation of the beta-adrenergic receptor. *J. Biol. Chem.* **1989**, *264*, 13572–13578.
- Karnik, S. S.; Sakmar, T. P.; Chen, H.-B.; Khorana, H. G. Cysteine residues 110 and 187 are essential for the formation of correct structure in bovine rhodopsin. *PNAS* **1988**, *85*, 8459–8463.
- Williamson, R. A.; Strange, P. G. Evidence for the Importance of a Carboxyl Group in the Binding of Ligands to the D2 Dopamine Receptor. *J. Neurochem.* **1990**, *55*, 1357–1365.
- Henderson, R.; Baldwin, J. M.; Ceska, T. A. Model for the Structure of Bacteriorhodopsin Based on High-resolution Electron Cryo-microscopy. *J. Mol. Biol.* **1990**, *213*, 899–929.
- Ovchinnikov, Y. A. Rhodopsin and bacteriorhodopsin: structure-function relationships. *FEBS Lett.* **1982**, *148*, 179–191.
- Dahl, S. G.; Edvardsen, O.; Sylte, I. Molecular dynamics of dopamine at the D2 receptor. *Proc. Natl. Acad. Sci. U.S.A.* **1991**, *88*, 8111–8115.
- Findlay, J.; Eliopoulos, E. Three-dimensional modelling of G protein-linked receptors. *Trends Pharmacol. Sci.* **1990**, *11*, 492–499.
- Hibert, M. F.; Trumpp-Kallmeyer, S.; Bruinvels, A.; Hoflack, J. Three-dimensional models of neurotransmitter G-binding protein-coupled receptors. *Mol. Pharmacol.* **1991**, *40*, 8–15.
- Livingstone, C. D.; Strange, P. G.; Naylor, L. H. Molecular Modelling of D2-like Dopamine Receptors. *Biochem. J.* **1992**, *287*, 277–282.
- Trumpp-Kallmeyer, S.; Hoflack, J.; Bruinvels, A.; Hibert, M. Modeling of G-Protein-Coupled Receptors: Application to Dopamine, Adrenaline, Serotonin, Acetylcholine, and Mammalian Opsin Receptors. *J. Med. Chem.* **1992**, *35*, 3448–3462.
- Zhang, D.; Weinstein, H. Signal Transduction by a 5-HT<sub>2</sub> Receptor: A Mechanistic Hypothesis from Molecular Dynamics Simulations of the Three-Dimensional Model of the Receptor Complexed to Ligands. *J. Med. Chem.* **1993**, *36*, 934–938.
- Teeter, M. M.; Roe, S. M.; Heo, N. H. The High Resolution (0.83 Å) Crystal Structure of the Hydrophobic Protein Crambin at 130K. *J. Mol. Biol.* **1993**, *230*, 292–311.
- Whitlow, M.; Teeter, M. M. An Empirical Examination of Potential Energy Minimization Using the Well-Determined Protein Crambin. *J. Am. Chem. Soc.* **1986**, *108*, 7163–7172.
- Whitlow, M.; Teeter, M. M. Tertiary Structure Prediction of Homologous Proteins:  $\alpha_1$  Purothionin and Viscotoxin A3 from Crambin. *J. Biomol. Str. Dyn.* **1985**, *2*, 831–848.
- Froimowitz, M.; Neumeyer, J. L.; Baldessarini, R. J. A Stereochemical Explanation of the Dopamine Agonist and Antagonist Activity of Stereoisomeric Pairs. *J. Med. Chem.* **1986**, *29*, 1570–1573.
- Froimowitz, M.; Baldessarini, R. J. A Stereochemical and Conformational Model of Dopaminergic Agonist and Antagonist Activity: Further Evaluation. *J. Pharm. Sci.* **1987**, *76*, 557–564.
- Froimowitz, M.; Råmsby, S. Conformational Properties of Semi-rigid Antipsychotic Drugs: The Pharmacophore for Dopamine D-2 Antagonist Activity. *J. Med. Chem.* **1991**, *34*, 1707–1714.
- Wikström, H.; Andersson, B.; Sanchez, D.; Lindberg, P.; Arvidsson, L.-E.; Johansson, A. M.; Nilsson, J. L. G.; Svensson, K.; Hjorth, S.; Carlsson, A. Resolved Monophenolic 2-Aminotetralins and 1,2,3,4,4a,5,6,10b-Octahydro-benzof[quinolines]: Structural and Stereochemical Considerations for Centrally Acting Pre- and Postsynaptic Dopamine-Receptor Agonists. *J. Med. Chem.* **1985**, *28*, 215–225.
- Liljefors, T.; Bøgesø, K. P. Conformational Analysis and Structural Comparison of (1R,3S)-(+)- and (1S,3R)-(-)-Tefludazine, (S)-(+)- and (R)-(-)-Octoclotheptin, and (+)-Dexaclamol in Relation to Dopamine Receptor Antagonism and Amine-Uptake Inhibition. *J. Med. Chem.* **1988**, *31*, 306–312.
- Froimowitz, M.; Cody, V. Biologically Active Conformers of Phenothiazines and Thioxanthenes. Further Evidence for a Ligand Model of Dopamine D2 Receptor Antagonists. *J. Med. Chem.* **1993**, *36*, 2219–2227.
- Kaiser, C.; Setler, P. E. Antipsychotic Agents. In *Burger's Medicinal Chemistry*; Wolff, M. E., Ed.; John Wiley: New York, 1981; pp 859–980.
- Neve, K. A. Regulation of dopamine D2 receptors by sodium and pH. *Mol. Pharmacol.* **1991**, *39*, 570–578.
- Neve, K. A.; Cox, B. A.; Henningsen, R. A.; Spanoyannis, A.; Neve, R. L. A pivotal role for aspartate-80 in the regulation of dopamine D2 receptor affinity for drugs and inhibition of adenylyl cyclase. *Mol. Pharmacol.* **1991**, *39*, 733–739.
- Horstman, D. A.; Brandon, S.; Wilson, A. L.; Guyer, C. A.; Cragoe, E. J.; Limbird, L. An aspartate conserved among G-protein receptors confers allosteric regulation of alpha2-adrenergic receptors by sodium. *J. Biol. Chem.* **1990**, *265*, 21590–21595.

- (36) Watanabe, M.; George, S. R.; Seeman, P. Regulation of anterior pituitary D2 dopamine receptors by magnesium and sodium ions. *J. Neurochem.* **1985**, *45*, 1842–1849.
- (37) Schertler, G. F. X.; Villa, C.; Henderson, R. Projection structure of rhodopsin. *Nature* **1993**, *362*, 770–772.
- (38) Branden, C.; Tooze, J. Introduction to Protein Structure. In *Book Introduction to Protein Structure*; Garland Publishing, Inc.: New York, 1991.
- (39) Seeman, P. Dopamine receptor sequences: therapeutic levels of neuroleptics occupy D2 receptors, clozapine occupies D4. *Neuropsychopharmacology* **1992**, *7*, 261–284.
- (40) Schiffer, M.; Edmondson, A. B. The use of the helical wheel to characterize amphipathic helices. *Biophys. J.* **1967**, *7*, 121–135.
- (41) Cannon, J. G. Chemistry of Dopaminergic Agonists. In *Advances in Neurology*; Calne, D. B., Chase, T. N., Barbeau, A., Eds.; Raven Press: New York, 1975; pp 177–183.
- (42) Tedesco, J. L.; Seeman, P.; McDermed. The Conformation of Dopamine at its Receptor: Binding of Momohydroxy-2-amino-tetralin Enantiomers and Positional Isomers. *Mol. Pharmacol.* **1979**, *16*, 369–381.
- (43) Abola, E.; Bernstein, R. C.; Bryant, S. H.; Koetzle, T. F.; Weng, J. Protein Data Bank. In *Crystallographic Databases – Information Content, Software Systems, Scientific Applications*; Allen, F. H., Bergerhoff, G., Sievers, R., Eds.; Data Commission of the International Union of Crystallography: Bonn/Cambridge/Chester, 1987; pp 107–132.
- (44) Bernstein, P. C.; Koetzle, T. F.; Williams, G. J. B.; Meyer, E. F.; Brice, M. D.; Rodgers, J. R.; Kennard, O.; Shimanouchi, T.; Tasumi, M. The Protein Data Bank. *J. Mol. Biol.* **1977**, *112*, 535–542.
- (45) Jones, T. A. Interactive Computer Graphics: FRODO. *Methods Enzymol.* **1985**, *115*, 157–171.
- (46) Sankararamkrishnan, R.; Vishveshwara, S. Characterization of proline-containing alpha-helices (helix F model of bacteriorhodopsin) by molecular dynamics study. *Proteins* **1993**, *15*, 26–41.
- (47) MacArthur, M. W.; Thornton, J. M. Influence of Proline Residues on Protein Conformation. *J. Mol. Biol.* **1991**, *218*, 397–412.
- (48) Ponder, J. W.; Richards, F. M. Tertiary Templates for proteins: use of packing criteria in the enumeration of allowed sequences for different structural classes. *J. Mol. Biol.* **1987**, *193*, 775–791.
- (49) Sack, J. S. CHAIN: A crystallographic modeling program. *J. Mol. Graph.* **1988**, *6*, 244–245.
- (50) Gao, Y.; Ram, V. J.; Campbell, A.; Kula, N. S.; Baldessarini, R. J.; Neumeyer, J. L. Synthesis and Structural Requirements of N-Substituted Norapomorphines for Affinity and Activity at Dopamine D-1, D-2, and Agonist Receptor Sites in Rat Brain. *J. Med. Chem.* **1990**, *33*, 39–44.
- (51) Wikström, H.; Andersson, B.; Elebring, T.; Svensson, K.; Carlsson, A.; Largent, B. N-Substituted 1,2,3,4,4a,5,6,10b-Octahydrobenzo[*f*]quinolines and 3-Phenylpiperidines: Effects on Central Dopamine and  $\sigma$  Receptors. *J. Med. Chem.* **1987**, *30*, 2169–2174.
- (52) Atkinson, E. R.; Bullock, F. J.; Granchelli, S. E.; Archer, S.; Rosenberg, F. J.; Teiger, D. G.; Nachode, F. C. Emetic activity of N-substituted norapomorphines. *J. Med. Chem.* **1975**, *18*, 1000–1003.
- (53) Tian, W.-N.; Deth, R. C. Precoupling of Gi/Go-linked receptors and its allosteric regulation by monovalent cations. *Life Sci.* **1993**, *52*, 1899–1907.
- (54) Jursic, B. S. Molecular Mechanics Calculation and Spectroscopic Determination of Enantiomeric Discrimination of Electron Rich Aromatic Racemic Compounds with Optically Pure Electron Poor Aromatic Amides. Abstracts of the 207th American Chemical Society National Meeting, San Diego, CA, March 13–18, 1994; Division of Organic Chemistry, No. 28.
- (55) Froimowitz, M.; Deng, Y.; Jacob, J. N.; Li, N.; Cody, V. Dopaminergic (4aR,10bS)-CIS- and (4aS,10bS)-trans-octahydrobenzo[*f*]quinolines have similar pharmacophores. *Drug Des. Disc.* **1994**, in press.
- (56) Baldwin, J. M. The Probable Arrangement of the Helices in G Protein-coupled Receptors. *EMBO J.* **1993**, *12*, 1693–1703.
- (57) Tomic, M.; Seeman, P.; George, S. R.; O'Dowd, B. F. Dopamine D1 Receptor Mutagenesis: Role of Amino Acids in Agonist and Antagonist Binding. *Biochem. Biophys. Res. Commun.* **1993**, *191*, 1020–1027.
- (58) Mansour, A.; Meng, F.; Meador-Woodruff, J. H.; Taylor, L. P.; Civelli, O.; Akil, H. Site-directed Mutagenesis of the Human Dopamine D2 Receptor. *Eur. J. Pharmacol.* **1992**, *227*, 205–214.
- (59) Strange, P. G. New Insights into Dopamine Receptors in the Central Nervous System. *Neurochem. Int.* **1993**, *22*, 223–236.
- (60) Strader, C. D.; Sigal, I. S.; Register, R. B.; Candelore, M. R.; Rands, E.; Dixon, R. A. F. Identification of Residues Required for Ligand Binding to the beta-Adrenergic Receptor. *Proc. Natl. Acad. Sci. U.S.A.* **1987**, *84*, 4384–4388.
- (61) Wang, C.-d.; Buck, M. A.; Fraser, C. M. Site-directed mutagenesis of alpha2a-adrenergic receptors: identification of amino acids involved in ligand binding and receptor activation by agonists. *Mol. Pharmacol.* **1991**, *40*, 168–179.
- (62) Wang, C.; Gallaher, T. K.; Shih, J. C. Site-Directed Mutagenesis of the Serotonin 5-Hydroxytryptamine2 Receptor: Identification of Amino Acids Necessary for Ligand Binding and Receptor Activation. *Mol. Pharmacol.* **1993**, *43*, 931–940.
- (63) Pollock, N. J.; Manelli, A. M.; Hutchins, C. W.; Steffey, M. E.; MacKenzie, R. G.; Frail, D. E. Serine Mutations in Transmembrane V of the Dopamine D1 Receptor Affect Ligand Interactions and Receptor Activation. *J. Biol. Chem.* **1992**, *267*, 17780–17786.
- (64) Nakayama, T. A.; Khorana, H. G. Mapping of the amino acids in membrane embedded helices that interact with the retinal chromophore in bovine rhodopsin. *J. Biol. Chem.* **1991**, *266*, 4269–4275.
- (65) Wess, J. Molecular Basis of Muscarinic Acetylcholine Receptor Function. *Trends Pharmacol. Sci.* **1993**, *14*, 308–313.
- (66) Choudhary, M. S.; Craig, S.; Roth, B. L. A Single Point Mutation (Phe340→Leu340) of a Conserved Phenylalanine Abolishes 4-[125I]Iodo-(2,5-dimethoxy)phenylisopropylamine and [3H]Mesulergine But Not [3H]Ketanserin Binding to 5-Hydroxytryptamine2 Receptors. *Mol. Pharmacol.* **1993**, *43*, 755–761.
- (67) Summers, R. J.; McMartin, L. R. Adrenoceptors and Their Second Messenger Systems. *J. Neurochem.* **1993**, *60*, 10–23.
- (68) Guan, X. M.; Peroutka, S. J.; Kobilka, B. K. Identification of a Single Amino Acid Residue Responsible for the Binding of a Class of Beta-Adrenergic Receptor Antagonists to 5-Hydroxytryptamine1A Receptors. *Mol. Pharmacol.* **1992**, *41*, 695–698.
- (69) Oksenberg, D.; Marsters, S. A.; O'Dowd, B. F.; Jin, H.; Havlik, S.; Peroutka, S. J.; Ashkenazi, A. A Single Amino-acid Difference Confers Major Pharmacological Variation between Human and Rodent 5-HT1B Receptors. *Nature* **1992**, *360*, 161–163.
- (70) Suryanarayana, S.; Kobilka, B. K. Amino Acid Substitutions at Position 312 in the Seventh Hydrophobic Segment of the beta2-Adrenergic Receptor Modify Ligand-Binding Specificity. *Mol. Pharmacol.* **1993**, *44*, 111–114.
- (71) Dohman, H. G.; Caron, M. G.; Strader, C. D.; Amlaiky, N.; Lefkowitz, R. J. Identification and Sequence of a Binding Site Peptide of the Beta2-Adrenergic Receptor. *Biochemistry* **1988**, *27*, 1813–1817.
- (72) Chanda, P. K.; Minchin, M. C. W.; Davis, A. R.; Greenberg, L.; Reilly, Y.; McGregor, W. H.; Bhat, R.; Iubeck, M. D.; Mizutani, S.; Hung, P. P. Identification of Residues Important for Ligand Binding to the Human 5-Hydroxytryptamine1A Serotonin Receptor. *Mol. Pharmacol.* **1993**, *43*, 516–520.
- (73) Zhou, W.; Flanagan, C.; Ballesteros, J. A.; Konvicka, K.; Davidson, J. S.; Weinstein, H.; Millar, R. P.; Sealfon, S. C. A reciprocal mutation supports helix 2 and helix 7 proximity in the gonadotropin-releasing hormone receptor. *Mol. Pharmacol.* **1994**, *45*, 165–170.
- (74) Kjelsberg, M. A.; Cotecchia, S.; Ostrowski, J.; Caron, M. G.; Lefkowitz, R. J. Constitutive activation of the alpha1B-adrenergic receptor by all amino acid substitutions at a single site. *J. Biol. Chem.* **1992**, *267*, 1430–1433.
- (75) Fraser, C. M. Site-directed mutagenesis of  $\beta$ -adrenergic receptors: identification of conserved cysteine residues that independently affect ligand binding and receptor activation. *J. Biol. Chem.* **1989**, *264*, 9266–9270.
- (76) Grigoriadis, D.; Seeman, P. The Dopamine/Neuroleptic Receptor. *Can. J. Neurol. Sci.* **1984**, *11*, 108–113.
- (77) Livingstone, C. D.; Strange P. G.; Naylor, L. H. Three dimensional models of the rat D2, D3, and D4 dopamine receptors. *Biochem. Soc. Trans.* **1992**, *20*, 148S.
- (78) Dohman, H. G.; Caron, M. G.; DeBlasi, A.; Frielle, T.; Lefkowitz, R. J. Role of Extracellular Disulfide-Bonded Cysteines in the Ligand Binding function of the Beta2-Adrenergic Receptor. *Biochemistry* **1990**, *29*, 2335–2342.
- (79) Kurtenbach, E.; Curtis, C. A. M.; Pedder, E. K.; Aitken, A.; Harris, A. C. M.; Hulme, E. C. Muscarinic acetylcholine receptors. Peptide sequencing identifies residues involved in antagonist binding and disulfide bond formation. *J. Biol. Chem.* **1990**, *265*, 13702–13708.
- (80) Fraser, C. M.; Wang, C.-D.; Robinson, D. A.; Gocayne, J. D.; Venter, J. C. Site-directed mutagenesis of m1 muscarinic acetylcholine receptors: conserved aspartic acids play important role in receptor function. *Mol. Pharmacol.* **1989**, *36*, 840–847.
- (81) Kao, H.-T.; Adham, N.; Olsen, M. A.; Weinsank, R. K.; Branchek, T. A.; Hartig, P. R. Site-directed mutagenesis of a single residue changes the binding properties of the serotonin 5-HT2 receptor from a human to a rat pharmacology. *FEBS Lett.* **1992**, *307*, 324–328.
- (82) Hoflack, J.; Trumpp-Kallmeyer, S.; Hibert, M. Re-evaluation of bacteriorhodopsin as a model for G protein-coupled receptors. *Trends Pharmacol. Sci.* **1994**, *15*, 7–9.
- (83) Noel, J. P.; Hamm, H. E.; Sigler, P. B. The 2.2 Å crystal structure of transducin-alpha complexed with GTP gamma S. *Nature* **1993**, *366*, 628–629 and 654–663.